

Wilson loops in 2D Yang Mills: Euler Characters and Loop equations

Sanjaye Ramgoolam

skr@genesis2.physics.yale.edu

Dept. of Physics

Yale University

New Haven, CT 06511

Abstract

We give a simple diagrammatic algorithm for writing the chiral large N expansion of intersecting Wilson loops in $2D$ $SU(N)$ and $U(N)$ Yang Mills theory in terms of symmetric groups, generalizing the result of Gross and Taylor for partition functions. We prove that these expansions compute Euler characters of a space of holomorphic maps from string worldsheets with boundaries. We prove that the Migdal-Makeenko equations hold for the chiral theory and show that they can be expressed as linear constraints on perturbations of the chiral $YM2$ partition functions. We briefly discuss finite N , the non-chiral expansion, and higher dimensional lattice models.

1. Introduction

We develop formulae for the chiral large N expansion of Wilson averages in 2D Yang Mills. This generalizes the results of Gross and Taylor [1] who expressed the chiral expansion of partition functions in terms of a sum of delta functions over symmetric groups. The generalisation of their result is best expressed in a diagrammatic form. This diagrammatic expression has a direct interpretation in terms of branched covers. The general structure of the diagram is understood in terms of elementary properties of the appropriate space of branched covers :

- (a) degrees of the maps in various regions of the target space and,
- (b) the fundamental groups of the target space and of the Wilson graph (see definition in section 4.1).

The detailed nature of the sums over symmetric group elements appearing is understood in terms of the counting of equivalence classes (definition in section 4.2) of the relevant class of branched covers, and from the conjecture (section 9 of ref [2]) that Wilson averages compute Euler characters of the space of branched covers.

In sections 2 and 3 we explain these ideas in the familiar cases of manifolds with and without boundary. In section 4 we introduce Wilson observables, associated to curves in the target Σ_T , and state the conjecture from [2] for the geometrical interpretation of their expectation values. We recall the proof of the conjecture for non-intersecting Wilson loops in section 5. Readers familiar with the string theory of 2D Yang Mills may prefer to move on to section 4 after reading the introduction. The main results of this paper are in sections 6, 8, 9, 11 and 12.

In section 6, we give the general algorithm for writing the chiral large N expansion. It uses words in the generators of the fundamental group of the Wilson graph, arranges them along strands labelled with positive integers, manipulates the strands via a simple diagrammatic move (see fig. 12), and constructs the final answer by replacing the generators with certain sums over permutations.

In section 7, this algorithm is derived from exact answers for 2D Yang Mills in terms of group integrals which were derived in [3,4,5]. In sections 8-10, we give the geometrical interpretation in terms of branched covers and Euler characters, using many ideas from [1] and [2]. We have adopted the words ‘braid diagrams’ for the diagrams which express the chiral large N expansions of Wilson averages. This terminology will be explained in section 7.1 and appendix A.

In this diagrammatic expression of Wilson averages, some surprising properties of Wilson averages become transparent. First we show that in the chiral theory the Wilson averages can be rather directly related to closed strings. We explain this in remarks in sections 5 and 8. Second we show in section 11 that the *chiral Wilson averages* satisfy the Migdal-Makeenko loop equations. Recall that the chiral expansion only gives part of the full $1/N$ expansion of $2D$ Yang Mills [1]: however from the string point of view it is an interesting theory. In fact, ref [2] constructs a string action for the chiral theory by localizing to spaces of holomorphic maps (as well as one for the non-chiral theory by localising to spaces of holomorphic + anti-holomorphic maps). The full large N expansion of YM_2 is the non-chiral (coupled) expansion. Standard proofs of Migdal-Makeenko imply that the coupled expansion for Wilson averages should satisfy the loop equations. The fact that chiral Wilson averages satisfy loop equations may have some mathematical interest since the chiral theory is the worldsheet field theory for classical Hurwitz spaces of branched covers. The third property concerns an analogy to 2D gravity. The loop equations are non-linear equations, but as in 2D gravity [6]: The non-linear loop equations can be used to derive linear constraints on perturbations of the partition function.

We will generally be dealing with the chiral $SU(N)$ theory. Occasionally, we will deal with the chiral zero charge sector of the $U(N)$ theory, which has the same structure as the chiral $SU(N)$ theory except for a small difference in the area dependent exponentials, and which has been studied, for example, in [1,7,8,9]. This will simplify some formulae in section 12.

In the final section, we have some general remarks on the application of this diagrammatic formalism for the geometry of large N group integrals to finite N YM_2 , non-chiral YM_2 and higher dimensional lattice models.

2. Partition function

The basic tool that leads to an interpretation of the chiral expansion of YM_2 , in terms of covering spaces and Euler characters of spaces of holomorphic maps (section 5 of [2]) is its expression in terms of delta functions over symmetric groups, which are related, by Riemann's theorem, to the counting of branched covers [1](for a review see [10]).

The main ingredient in the derivation of the chiral expansion from exact results for the partition function [5,3,4] is Schur-Weyl duality, which we describe briefly. All unitary irreps of $SU(N)$ are obtained from reducing tensor products of the fundamental rep V

(for $U(N)$ we need tensor products of both the fundamental and its complex conjugate). Consider the action of $SU(N)$ on $V^{\otimes n}$. Let $\rho(U)$ represent the action of U in $V^{\otimes n}$. The symmetric group S_n acts on $V^{\otimes n}$ by permuting the factors. Let $\tilde{\rho}$ be the map from S_n to $End(V^{\otimes n})$. So

$$\tilde{\rho}(\sigma)|e_{i_1} > \otimes |e_{i_2} > \otimes \cdots |e_{i_n} > = |e_{i_{\sigma(1)}} > \otimes |e_{i_{\sigma(2)}} > \otimes \cdots |e_{i_{\sigma(n)}} > . \quad (2.1)$$

Schur-Weyl duality: The commutant of $\rho(SU(N))$ in $V^{\otimes n}$ is $\tilde{\rho}(\mathbb{C}(S_n))$, and $V^{\otimes n}$ is completely reducible, as a representation of $SU(N) \times S_n$, to $V^{\otimes n} \cong \sum_Y R(Y) \otimes r(Y)$.

In the $SU(N)$ theory irreps can be labelled by Young diagrams with fewer than N rows: $Y \in \mathcal{Y}_n^{(N)}$, where $\mathcal{Y}_n^{(N)}$ is the set of valid Young diagrams for $SU(N)$. For $N > n$ (which is relevant in the large N expansions), $\mathcal{Y}_n^{(N)} = \mathcal{Y}_n$, the set of all Young diagrams with n boxes. We denote by $R(Y)$ ($r(Y)$) the irrep of $SU(N)$ (S_n) corresponding to Y . So if P_Y is the Young projector for the rep of S_n associated with Y , we have [11]

$$P_Y V^{\otimes n} \cong R(Y) \otimes r(Y). \quad (2.2)$$

We recall the result for the chiral partition function, for a target Riemann surface Σ_T of genus G and area A , as an expansion in terms of symmetric group quantities :

$$\begin{aligned} Z(G, A, N) &= \sum_{n=0}^{\infty} \left[\frac{1}{n!} \delta_n \left(e^{-\frac{nA}{2} - A \frac{T_2^{(n)}}{N} + \frac{A(n^2)}{2N^2}} N^{n(2-2G)} \Omega_n^{2-2G} \prod_{j=1}^G \sum_{s_j, t_j \in S_n} s_j t_j s_j^{-1} t_j^{-1} \right) \right]. \end{aligned} \quad (2.3)$$

Here

$$\Omega_n = \sum_{v \in S_n} v N^{K_v - n} = N^{-n} \sum_{v \in S_n} v tr_n(\tilde{\rho}(v)), \quad (2.4)$$

where tr_n is the trace in $V^{\otimes n}$. The $n = 0$ term in (2.3) is defined to be 1. $T_2^{(n)}$ is an element in the group algebra of S_n , equal to the sum of all the transpositions. The delta function δ_n acting on the group algebra of S_n evaluates the coefficient of the identity permutation. The omega factors were expanded out in [2] producing words in the free algebra generated by elements of S_n , $\mathcal{F}(S_n)$. Each permutation comes with a power of N which is $N^{K_\sigma - n}$. All words of length L are weighted by the Euler character of the configuration space of L points on Σ_T . This uses the fact the power of Ω_n is exactly the Euler character of the target

space. By Riemann's theorem, the sums over symmetric groups count branched covers (holomorphic maps) of degree n , weighted by the inverse of the order of the automorphism group. Using the fibration of Hurwitz space over configuration spaces leads to the result that the zero area partition function is the generating function of Euler characters of the space of holomorphic maps from a smooth worldsheet Σ_W onto the target Σ_T . The detailed discussion is in [2]. For finite area we have a similar structure: elements in $\mathcal{F}(S_n)$, weighted by A dependent *power series* in $1/N$. For the geometrical interpretation in terms of branched covers, the factor $e^{-A \frac{T_2^{(n)}}{N}}$ is expanded out to give sums of transpositions. Terms with these sums are interpreted as contributions from maps which have some number of simple branch points weighted by factors of the area. The term $e^{\frac{-n^2 A}{2N^2}}$ is also expanded out and interpreted as contributions from maps involving worldsheets with double points and collapsed handles [12,1].

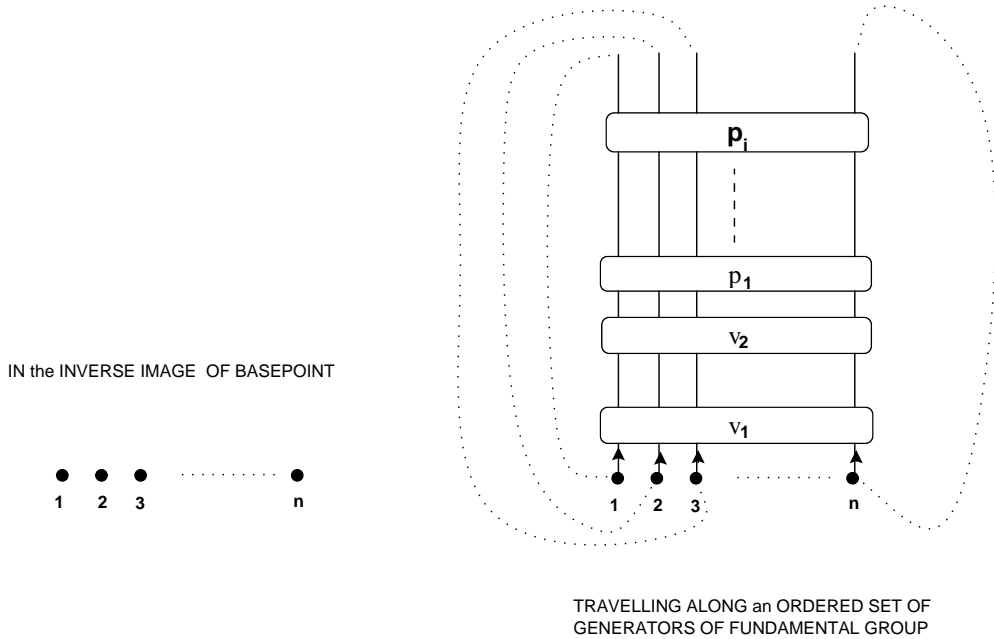


Fig. 1: Pictorial representation of delta function for partition function

Each term contributing to the partition function is a sequence of permutations which multiply to 1. Such a sequence can be expressed as in fig. 1, where we have drawn a typical term for $G = 0$. The v 's come from the Ω_n factors and the p_i 's come from the $AT_2^{(n)}$ term in the exponential. At the base of the diagram are n points labelled from 1 to

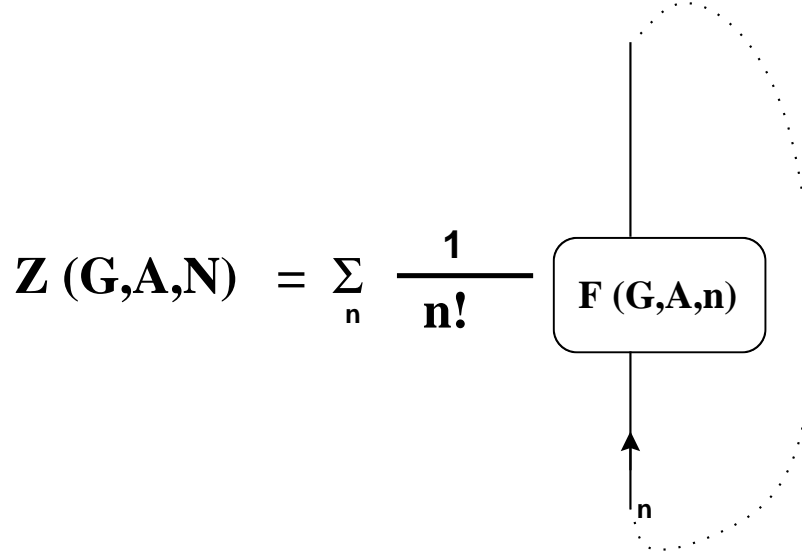


Fig. 2: Simplified pictorial representation for partition function

n . They correspond to the n points in the inverse image of an arbitrarily chosen basepoint, y_0 , on the target Σ_T . For each generator of the fundamental group $\Sigma_T - \{\text{branch points}\}$ the diagram contains a permutation, which may be thought more pictorially in terms of the strands winding around each other according to the permutation. The product of the permutations read from top to bottom is equal to the identity. This is expressed by the dotted lines which join top to bottom with no further winding. In fig. 2, we draw a simplified version of the diagram with the whole sequence of permutations written as one F factor.

$$F(G, A, n) \in \mathcal{F}(S_n) \otimes \mathbb{R}(1/N)$$

$$= e^{-\frac{nA}{2} - A\frac{T_2^{(n)}}{N} + \frac{n^2 A}{2N^2}} N^{n(2-2G)} \Omega_n^{2-2G} \prod_{i=1}^G \sum_{s_i, t_i \in S_n} s_i t_i s_i^{-1} t_i^{-1}. \quad (2.5)$$

After multiplying out the permutations, F determines an element of $\mathbb{Z}(S_n) \otimes \mathbb{R}(1/N)$.

The permutations can be represented in the standard way in tensor space, as operators in $\text{End}(V^{\otimes n})$. The identity permutation maps to the identity operator, so the delta function is equal to a delta function on the corresponding operators in tensor space. Observing that

$$\text{tr}_n(\tilde{\rho}(\sigma)) \equiv \text{tr}_n(\sigma) = N^{K_\sigma} = \delta_n(\sigma N^n \Omega_n), \quad (2.6)$$

we can also write Z very simply as a sum over traces in $V^{\otimes n}$:

$$Z(G, A, N) = \sum_n \frac{1}{n!} \text{tr}_n(F_n(G, A, N) \Omega_n^{-1} N^{-n}) \quad (2.7)$$

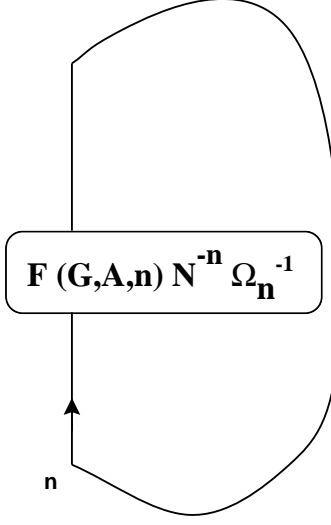
$$\mathbf{Z}(\mathbf{G}, \mathbf{A}, \mathbf{N}) = \sum_{\mathbf{n}} \frac{1}{\mathbf{n}!} \text{Tr} \left(\mathbf{F}(\mathbf{G}, \mathbf{A}, \mathbf{n}) \mathbf{N}^{-\mathbf{n}} \Omega_{\mathbf{n}}^{-1} \right)$$


Fig. 3: Partition function as a trace in tensor space.

This can be represented pictorially by replacing the dotted lines with solid lines, which indicate contracted indices, as in fig. 3.

3. Manifolds with boundary.

3.1. Hurwitz spaces for manifolds with boundary.

For target spaces with boundary, $(\Sigma_T, \partial\Sigma_T)$, chiral YM_2 partition functions are generating functions for Euler characters of spaces of branched covers from manifolds with boundary, $(\Sigma_W, \partial\Sigma_W)$, to the target space.

Definition 3.1. A *boundary-preserving branched covering* is a map

$$f : (\Sigma_W, \partial\Sigma_W) \rightarrow (\Sigma_T, \partial\Sigma_T) \quad (3.1)$$

such that

1. $f : \partial\Sigma_W \rightarrow \partial\Sigma_T$ is a covering map.
2. $f : \Sigma_W - \partial\Sigma_W \rightarrow \Sigma_T - \partial\Sigma_T$ is an orientation preserving branched covering.

Definition 3.2 Two maps f_1 and f_2 are said to be *equivalent* if there is a homeomorphism $\phi : \Sigma_W \rightarrow \Sigma_W$, such that $f_1 = f_2 \circ \phi$. An *automorphism* of a boundary-preserving branched cover is a homeomorphism ϕ such that $f = f \circ \phi$.

By (1) f determines a class \vec{k}_Γ for each component Γ of $\partial\Sigma_T$: $\vec{k}_\Gamma^{(j)}$ is the number of circles of winding number j in the inverse image of Γ . Let us assume that $\Sigma_T - \partial\Sigma_T$ is

connected. Then, by (2) f determines a branch locus $S(f) \subset \Sigma_T - \partial\Sigma_T$, an index n , and an equivalence class of a homomorphism $\psi_f : \pi_1(\Sigma_T - S(f), y_0) \rightarrow S_n$. We have the direct analog of Riemann's theorem:

Proposition 3.3. Let Σ_T be a connected, closed surface with boundary. Let $S \subset \Sigma_T - \partial\Sigma_T$ be a finite set, and let n be a positive integer. There is a one-one correspondence between equivalence classes of boundary-preserving branched covers (3.1) with branch locus S and equivalence classes of homomorphisms $\psi : \pi_1(\Sigma_T - S(f), y_0) \rightarrow S_n$.

The proof is in section 9 of [2]. Given the homomorphism we can construct a branched cover, and given a branched cover, we can obtain a homomorphism by lifting paths which generate the fundamental group [13]. The boundaries can be shrunk to give a surface with deleted points. So the counting of boundary preserving branched covers is related to a classical problem: that of counting branched covers with specified monodromies at the deleted points.

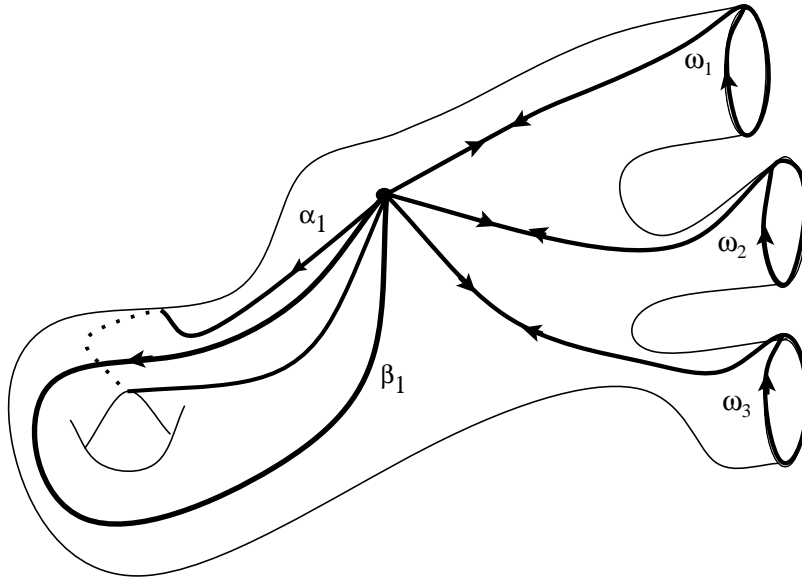


Fig. 4: Generators of fundamental group for manifold with boundary.

3.2. YM_2 partition functions for Manifolds with boundary

The partition function for a manifold of genus G , area A , with b boundaries, with specified holonomies U_1, \dots, U_b , is given by [3], [4],

$$Z(G, A, b; U_1, U_2, \dots, U_b) = \sum_R (\dim R)^{2-2G-b} e^{-\frac{A}{2N} C_2(R)} \chi_R(U_1) \cdots \chi_R(U_b). \quad (3.2)$$

We can consider expectation values of $\chi_{R_i}(U_i^\dagger)$ inserted at the i' th boundary. They are given by

$$\begin{aligned} Z(G, A, b; R_1, R_2, \dots R_b) &= \prod_{i=1}^b \int dU_i Z(G, A, b; U_1, U_2, \dots U_b) \prod_{i=1}^b \chi_{R_i}(U_i^\dagger) \\ &= \sum_R (\dim R)^{2-2G-b} e^{-\frac{AC_2(R)}{2N}} \delta_{R_1, R} \delta_{R_2, R} \dots \delta_{R_b, R}. \end{aligned} \quad (3.3)$$

A more direct string interpretation is obtained for insertions of certain linear combinations of the irreducible characters, called *loop functions*, $\Upsilon_{\vec{k}}(U)$, which depend on a *winding vector* \vec{k} . \vec{k} is a vector with an infinite number of components, most of which are zero. The vector \vec{k} determines a conjugacy class $[\vec{k}]$ of permutations with k_1 cycles of length 1, k_2 cycles of length 2 etc. , in $S_{n(\vec{k})}$, where $n(\vec{k}) = \sum_j j k_j$. If σ is a permutation in the class $[\vec{k}]$,

$$\begin{aligned} \Upsilon_{\vec{k}}(U) &= \Upsilon_{\sigma}(U) \\ &= \text{tr}_n(\sigma U) \\ &= \sum_{Y \in Y_n} \chi_{r(Y)}(\sigma) \chi_{R(Y)}(U), \end{aligned} \quad (3.4)$$

where the last equality follows directly from Schur-Weyl duality.

Insertion of the loop function into the path integral yields:

$$\begin{aligned} Z(G, A, b; \vec{k}_1, \vec{k}_2, \dots \vec{k}_b) &= \int dU_1 dU_2 \dots dU_b Z(G, A, b; U_1, U_2, \dots U_b) \prod_{i=1}^b \sum_{u_i \in [\vec{k}_i]} \frac{1}{n_i!} \Upsilon_{u_i}(U_i^\dagger) \\ &= \sum_n \sum_{u_1, \dots u_b} \frac{1}{n!} \delta(F(G, A, b, n) u_1 \dots u_b) \delta_{n_1, n} \delta_{n_2, n} \dots \delta_{n_k, n} \quad , \end{aligned} \quad (3.5)$$

where $F(G, A, b, n)$ is given by

$$\begin{aligned} F(G, A, b, n) &= \\ &= e^{-nA/2 - AT_2^{(n)} + \frac{n^2 A}{2N^2}} N^{n(2-2G-b)} \Omega_n^{2-2G-b} \prod_{j=1}^G \sum_{s_j, t_j \in S_n} s_j t_j s_j^{-1} t_j^{-1}. \end{aligned} \quad (3.6)$$

This formula can be derived by manipulations similar to those leading to the derivation of (2.3) [1]. Note that we need the insertion $\sum_{\sigma_i \in [\vec{k}_i]} \frac{1}{n_i!} \Upsilon_{\sigma_i}(U_i^\dagger) = \frac{||[\vec{k}_i]||}{n(\vec{k}_i)!}$ (where $||[\vec{k}_i]||$ is the number of elements in the conjugacy class $[\vec{k}_i]$), in order to make sure that we are counting equivalence classes of branched covers weighted by the inverse of the automorphism.

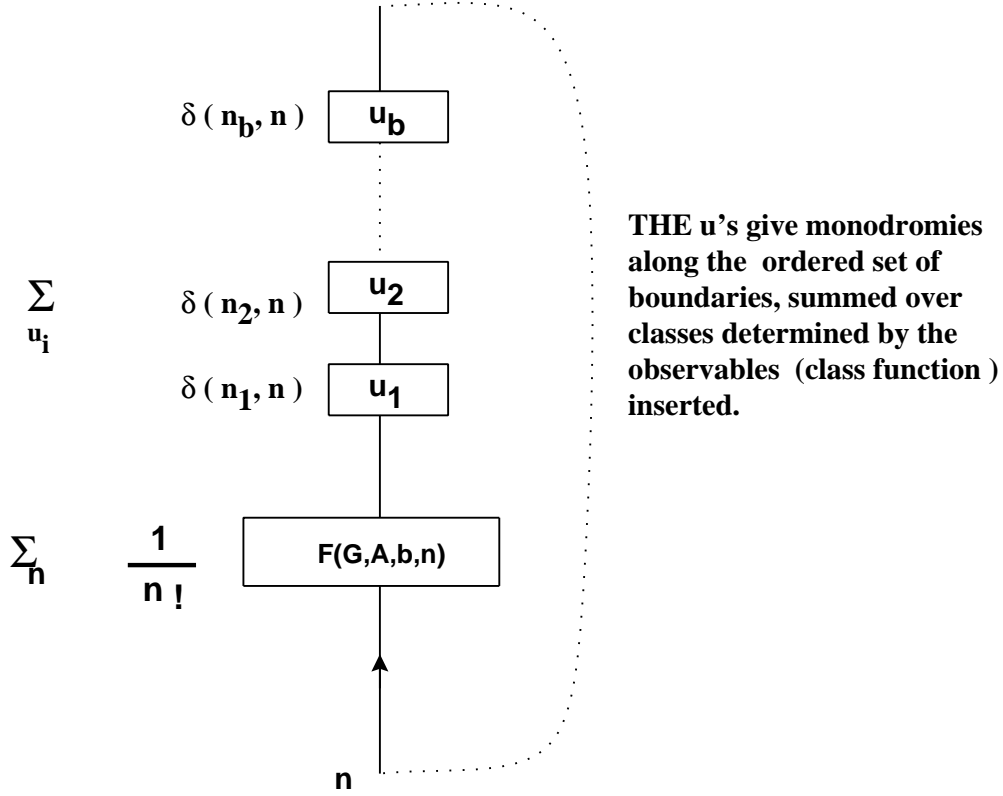


Fig. 5: Delta function for Manifold with Boundary

Again the delta function can be presented pictorially as in fig. 5. It expresses the fact that each term is obtained from a sequence of permutations obtained by travelling around cycles in the interior of the manifold (collected in the F factor), and around the boundaries, which all multiply to 1.

At $A = 0$ the partition function counts Euler characters of the space of branched covers where the map from worldsheet boundaries to the i 'th target boundary is in the homotopy class given by \vec{k}_i . To see this we expand the omega factors to generate arbitrary numbers of branch points, as for the chiral partition function. Note that the power of omega is appropriate for producing the Euler character of configuration spaces of points on Σ_T .

4. Wilson loops —observables and maps

4.1. Observables and exact answers

Wilson averages are computed by inserting in the path integral, traces of holonomies around specified paths. Each path Γ is a map from S^1 to the target space Σ_T . The

image of such a map is called \mathcal{G} . In general we have $\Pi S^1 \rightarrow \Pi \mathcal{G}$. We will call $\Pi \mathcal{G}$ the *Wilson graph*, which is made of a union of open edges and vertices. It may be connected or disconnected. For non-intersecting Wilson loops, the Wilson graph is a disjoint union of circles. The observable associated with it is

$$W_{R_\Gamma} = \text{tr}_{R_\Gamma} \left(\text{Pexp} \int_\Gamma A \right),$$

the trace in rep R_Γ of the holonomy of the gauge field along Γ . As in the case of manifolds with boundary, insertions of the appropriately normalised $\Upsilon_{\vec{k}_\Gamma}(U_\Gamma^\dagger)$ will have a more direct geometrical interpretation.

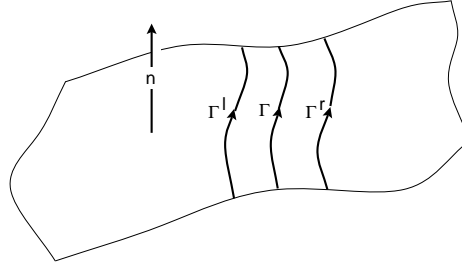


Fig. 6: Using the orientation of the surface and of the Wilson line we can define two infinitesimal deformations of the Wilson line Γ^l and Γ^r .

Using the orientation of Σ_T we can perturb each oriented Wilson loop Γ to its left or right, into loops Γ^l and Γ^r .

Witten [3] and Rusakov [4] wrote exact answers for the Wilson averages in terms of sums over representations and group integrals. Given a collection of curves $\{\Gamma\}$ on Σ_T , we have a decomposition into disjoint connected open components:

$$\Sigma_T - \Pi \mathcal{G} = \Pi_c \Sigma_T^c. \quad (4.1)$$

The component Σ_T^c has G_c handles, area A_c and b_c boundaries. A choice of orientation of the manifold Σ_T induces an orientation on each component. Assign to each oriented edge e of the Wilson graph a group element U_e . Each region induces on its boundaries an orientation. Any oriented boundary of a region can be expressed as a word in the edge paths and is assigned a group element equal to the corresponding product of edge variables. For each region there is a local factor equal to :

$$Z_c = \sum_{R_c} \dim R_c e^{-A_c C_2(R_c)/2} \prod_{i=1}^{b_c} \chi_{R_c}(U_c^{(i)}), \quad (4.2)$$

where $U_c^{(i)}$ is the holonomy around the i 'th oriented boundary of Σ_T^c . The full answer is

$$\langle \prod_{\{\Gamma\}} W_{R_\Gamma} \rangle = \sum_{R_c} \int \prod_e dU_e \prod_c Z_c \prod_\Gamma \chi_{R_\Gamma}(U_\Gamma^\dagger). \quad (4.3)$$

If we insert $\Upsilon_{\vec{k}_\Gamma}(U_\Gamma^\dagger)$, then we have instead of irreducible characters, the loop functions in the product over Γ .

Witten [3] also showed that these exact answers can be written as a sum over reps associated with each region, together with six j symbols associated with the vertices. In the case of non-intersecting Wilson averages, everything can be written in terms of sums over reps and fusion numbers.

4.2. Geometrical conjecture

In [2] there was a simple conjecture, based on results of [1], for interpreting the expectation values of all Wilson averages in the zero area limit in terms of Euler characters. Consider the insertion of $\prod_\Gamma \Upsilon_{\vec{k}_\Gamma}$. Elaborating the conjecture of [2], we have,

CONJECTURE 4.1 . The string interpretation for chiral Wilson loop amplitudes on Σ_T is obtained by imposing on branched covers $f : (\Sigma_W, \partial\Sigma_W) \rightarrow (\Sigma_T)$ the boundary condition that $f : \partial\Sigma_W \rightarrow \Pi\mathcal{G}$ is in the homotopy class

$$\partial\Sigma_W \xrightarrow{\{\vec{k}_\Gamma\}} \Pi_\Gamma S^1 \xrightarrow{\Pi\Gamma} \Pi\mathcal{G}. \quad (4.4)$$

The worldsheet and target are oriented. The worldsheet boundary has orientation compatible with that of worldsheet. The maps are orientation preserving. The first arrow describes a covering of oriented circles by oriented circles. The second is the homotopy class of the curves defining the Wilson loops.

Equivalences of such maps are defined as in Def 3.2 . Spaces of such maps will be called Hurwitz-Wilson spaces. More precisely we expect that Wilson averages are generating functions for orbifold Euler characters of Hurwitz-Wilson spaces.

To compactify the space of branched covers we will *allow branch points to lie on the Wilson graph*¹ . For a map with branch points on the graph, the image of the boundary $\partial\Sigma_W$ is deformed away from the branch point to the right of the oriented Wilson loop.

¹ The idea of letting the branch locus intersect the Wilson graph has also appeared in work of Kostov [14].

The image of the deformed Wilson loops is an infinitesimal deformation $\Pi\mathcal{G}'$ of the graph $\Pi\mathcal{G}$. With these prescriptions, the worldsheets are *always smooth* and the lifts of curves in the target space to the worldsheet boundary are unambiguously defined. ♠

The conjecture was proved for non-intersecting Wilson loops in [2]. The first main result of this paper is to prove it for intersecting loops.

The proof will involve a derivation of the chiral large N expansion in the form of a delta function over symmetric groups, using exact answers of [3] and [4]. The answers are expressed in a diagrammatic form, which simply generalises the diagrams we introduced in sections 2 and 3. We hope to have given sufficient detail, in sections 5-9, to convince the reader that the geometric properties alone determine the chiral zero area expansions.

5. Non-intersecting Wilson Loops

5.1. Covering space geometry

We describe some implications of conjecture 3.1 when the Wilson loops are non-intersecting. The worldsheets contributing to the Wilson loop expectation value have boundaries which map to the Wilson graph according to the specified conjugacy classes. For a map satisfying this condition, there can still be in the inverse image of the Wilson graph, curves which are not at the boundary of the worldsheet Σ_W , but in the interior.

Inside each component Σ_T^c , the maps restrict to branched covers. In the inverse image of each Wilson line there are $|\vec{k}_\Gamma| = \sum_j k_\Gamma^{(j)}$ circles which are worldsheet boundaries. The map from this union of circles is determined by the vector \vec{k}_Γ : there are $k_\Gamma^{(j)}$ circles which map with winding number j , so that the number of points belonging to worldsheet boundaries in the inverse image of each point on a Wilson line Γ , is $n(\vec{k}_\Gamma) = m_\Gamma$. There can be an arbitrary number of circles which are in the interior of the worldsheet. Since the map has to be orientation preserving on the components, Σ_T^c , and on the boundaries, the degree of the map is higher to the left of Γ . We have:

$$n(c_\Gamma^l) = n(c_\Gamma^r) + m_\Gamma, \quad (5.1)$$

as illustrated in fig. 7.

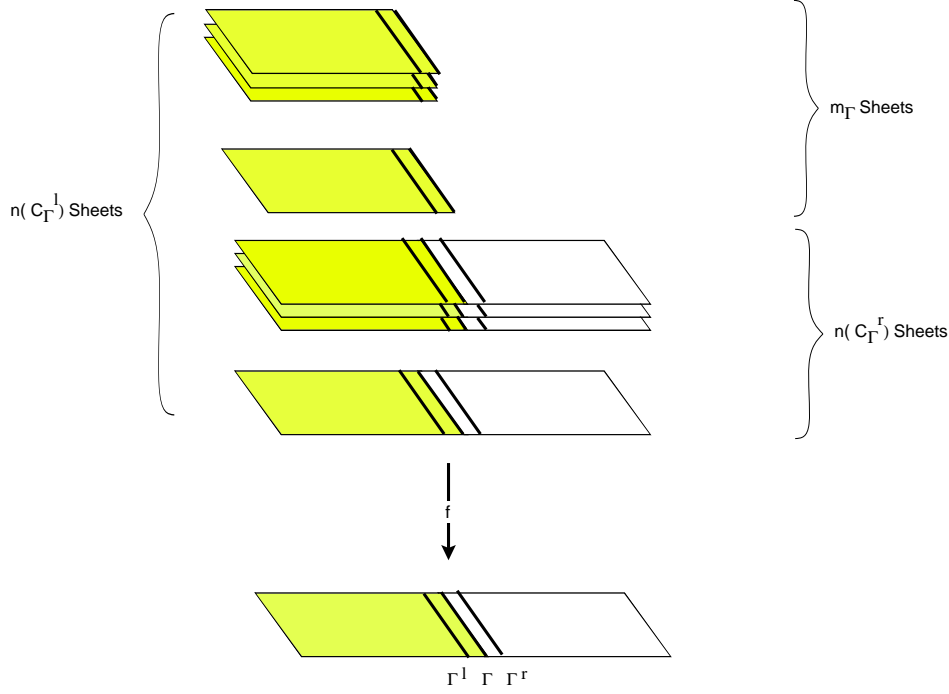


Fig. 7: Locally the covering map looks like this. Above Γ^r there are only interior curves. Above Γ^l there are interior and boundary curves.

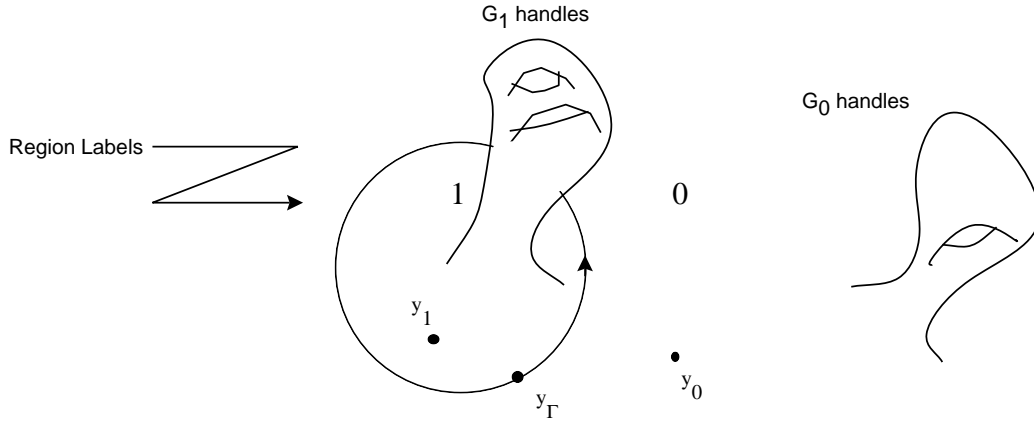


Fig. 8: Figure showing Wilson loop on sphere with handles attached : Gluing condition relates permutations seen from different basepoints

5.2. Description in terms of homomorphisms into symmetric groups

We can apply ideas from the theory of branched covers to count equivalence classes of these maps in terms of homomorphisms into symmetric groups. This is done formally and for any non-intersecting Wilson loop in [2]. We will summarise the main points here,

as applied to the example of a single non-intersecting loop, on a sphere with G_1 handles attached to region 1 on the left and G_0 handles attached to region 0 on the right (fig. 8). From (5.1) we have

$$n_1 = n_0 + m_\Gamma. \quad (5.2)$$

Given any map onto Σ_T of the kind in Conjecture 4.1, we can construct a sequence of permutations satisfying some conditions. Choose a basepoint y_c in region Σ_T^c , and label the n_c points in its inverse image. By lifting paths in non-trivial homotopy classes in each region, we pick up permutations satisfying a condition:

$$v_1(c) \cdots v_{L_c}(c) \prod_{i=1}^{G_c} [s_i(c), t_i(c)] u_c^{-1} = 1. \quad (5.3)$$

The v_i are permutations representing paths which wrap around branch points (at zero area they come from expanding the Ω_{n_c} factors), the s_i, t_i represent paths around the handles; u_1, u_0 are permutations along Γ as seen from a basepoint in the regions 0 or 1.

There are additional gluing conditions across each Wilson line, since the permutation of all the sheets in the inverse image of the Wilson line can be described in two ways. Approaching from the left (with more sheets) there is a permutation $u_1 \in S_{n_1}$ obtained by using the basepoint in region 1. Choose a basepoint y_Γ on the Wilson line. We also choose a path from y_0 to y_Γ and label the endpoints 1 to n_0 : then we label the remaining m_Γ points (which lie on worldsheet boundaries) $n_0 + 1$ to $n_0 + m_\Gamma = n_1$. We can combine u_0, σ_Γ into a permutation in S_{n_1} . These are equivalent ways of describing the same permutation from the point of view of two basepoints, so they must be related by a conjugation in S_{n_1} . We have the second gluing condition at each Wilson line: there must exist $\gamma \in S_{n_1}$ such that

$$u_1 = \gamma u_0 \sigma_\Gamma \gamma^{-1}. \quad (5.4)$$

This permutation γ is obtained by lifting a path connecting y_1 to y_Γ .

Conversely given a set of permutations satisfying the above conditions we can reconstruct the cover. First construct covers of the regions 0 and 1, following [13]: Cut open the target along the generators of $\pi_1(\Sigma_T^c - \text{branch points})$ and take n_c labelled copies of this cut surface. Glue according to the permutations v_c, s_c, t_c etc. Next, glue together regions 0 and 1 along the common boundary \mathcal{G} , and correspondingly glue together the covering surfaces according to the permutation γ . This means that the i 'th sheet on the left is glued to the $\gamma(i)$ 'th on the right.

Equivalent covers which are related by a homeomorphism ϕ such that $f_1 = f_2 \circ \phi$, lead to permutations which are related by conjugations, and there is a 1 – 1 correspondence between equivalence classes of covers and equivalence classes of permutations describing the covers (see [2]).

5.3. Chiral non-intersecting Wilson loops— qcd answers and geometric interpretation

We will now write the YM_2 answer for this Wilson loop and then express it in a diagrammatic form from which the covering space geometry can be read off. This exercise will be useful in understanding the more complicated intersecting Wilson loops.

$$\begin{aligned}
\left\langle \frac{|T_{\vec{k}_\Gamma}|}{m_\Gamma!} \Upsilon(\vec{k}_\Gamma, \Gamma) \right\rangle &= \sum_{n_0, n_1} \sum_{u_1 \in S_{n_1}} \sum_{u_0 \in S_{n_0}} \delta_{n_1, n_0+m} \\
&\frac{1}{n_1!} \frac{1}{n_0!} \delta(F_1(n_1)u_1^{-1}) \delta(F_0(n_0)u_0^{-1}) \delta(\gamma u_1 \gamma^{-1}(u_0 \cdot \sigma_\Gamma)) \\
&= \sum_{n_1, n_0} \frac{1}{n_1!} \frac{1}{n_0!} \delta(\gamma F_1(n_1) \gamma^{-1} F_0(n_0) \cdot \sigma_\Gamma)
\end{aligned} \tag{5.5}$$

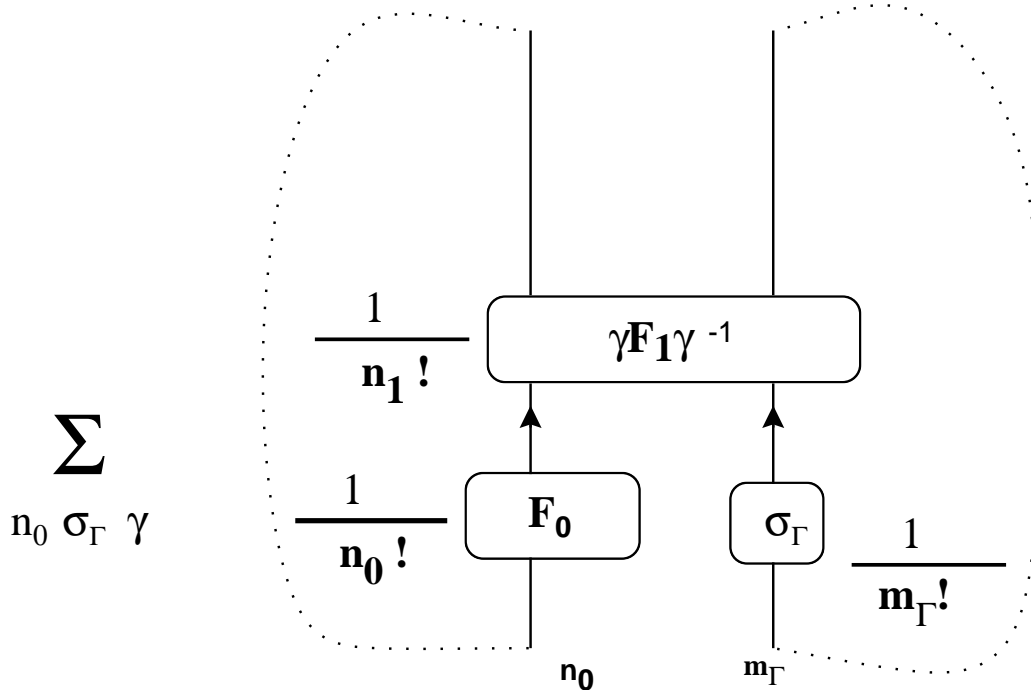


Fig. 9: Delta function for single chiral nonintersecting Wilson loop.

We recognize the first expression from (5.3) and (5.4). In the second expression, we have done the sums over u_1 and u_0 to get a simple formula, which still can be interpreted geometrically. We can express this in diagrammatic form (fig. 9) as we did for the partition function for manifolds with and without boundary.

The F_0 factor acts on the first n_0 numbers (which correspond to the inverse image of a point on the Wilson graph). It gives permutations representing branch points or non-trivial loops around handles in region 0. F_1 contains permutations obtained by lifting closed paths starting from the basepoint in region 1. Since the degree of the map in region 1 is n_1 , all the n_1 integers in the diagram can be permuted by F_1 . The conjugated F_1 gives monodromies obtained from the basepoint on the Wilson loop. Restricting the delta function to the first n_0 numbers, we see that they label points lying on sheets covering the target over both regions 0 and 1. After picking up permutations along all the generators of π_1 we get a trivial path, which is mapped to 1: following the lifts starting from each of the n_0 points, of all the generators of π_1 associated with cycles in regions 0 and 1, we get the trivial permutation. Restricting the delta function to the last m_Γ numbers we see that they correspond to sheets covering region 1 only, as they are only acted on by F_1 . The product of paths around the branch points in region 1 and the appropriate commutators for the handles in region 1 is homotopic to a path around the Wilson loop. So travelling along the inverse of the Wilson loop and then along all the non-trivial paths in region 1, we get the identity in π_1 which maps to the identity permutation. This is exactly the condition we read off by restricting to the m_Γ strands.

Note that we may construct the covers by starting with a cover of constant degree $n_0 + m_\Gamma$ of the whole surface Σ_T . In region 0, the first n_0 sheets can receive arbitrary permutations from the branchpoints etc. coming from the F_0 factors. The last m_Γ are permuted by a single branch point whose cycle structure is $[\vec{k}_\Gamma]$. To get the correct degree in each region, we cut out the m_Γ sheets from the outside. This construction gives the same kind of cover as that discussed in the previous subsection. The role of the branch point in the outside region permuting the m_Γ sheets is to produce the correct winding of the Wilson loop. These ideas will be useful in the intersecting case.

The above discussion shows that the discrete data (sums over permutations) which enter the Wilson average count covers predicted by conjecture 4.1. To see that we get Euler characters, of these spaces we use the fact that the F_c factors contain $\Omega_{n_c}^{\chi(\Sigma_T^c)}$. Thus contributions with L_c branch points in Σ_T^c are weighted by $\prod_c \chi(\Sigma_T^c, L_c)$, the product of Euler characters of configuration spaces of L_c points in Σ_T^c . Using the fibration of

Hurwitz-Wilson spaces over configuration spaces shows that we have Euler characters of these spaces.

Remarks : a) In the case of non-intersecting loops the Euler character of the space of branched covers is the same whether or not the branch points can lie on the Wilson graph. This is because the Wilson graph has Euler character zero in this case. A consequence is that the delta functions contain Ω factors only inside the F factors for the different regions. This will no longer be true in the intersecting case, where there will be extra Ω factors.

b) **Relation to closed strings.** If we multiply the Wilson insertion by $N^{|\vec{k}_\Gamma| - 2m_\Gamma G_0}$, the Wilson average has the interpretation of counting covers of constant degree with the permutations having some special structure (given by the delta function). So Chiral Wilson averages compute Euler characters of subspaces of ordinary Hurwitz spaces.

6. Algorithm for computing the chiral expansion for arbitrary Wilson Loops

In this section, we will show how to construct a delta function when the Wilson graph is a connected one living on a sphere with G_c handles attached to Σ_T^c . The generalisation is simple (see comment at the end of this section).

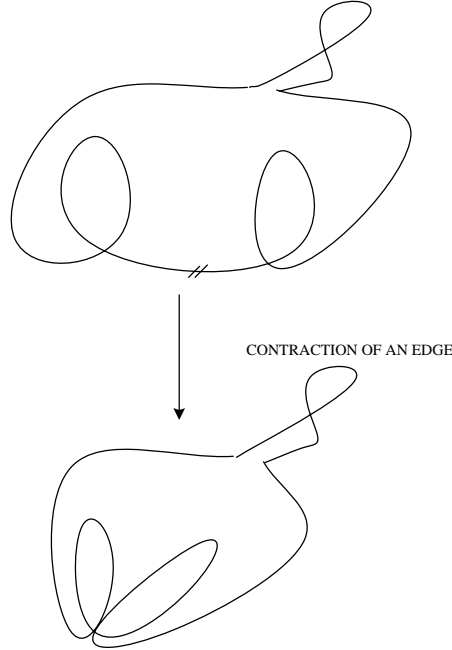
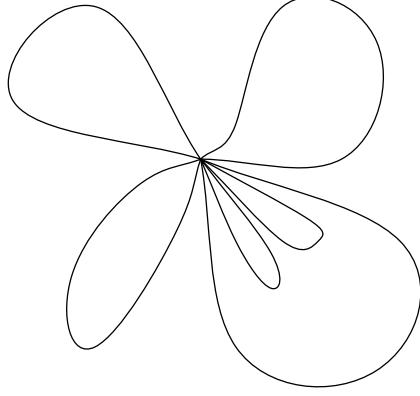


Fig. 10: Edge contraction does not change the fundamental group.



A flower

Fig. 11: Fundamental group of flower is a free group.

We first express the Wilson loops $\{\Gamma\}$ in terms of the fundamental group of the Wilson graph. A set of generators of the Wilson graph can be written down in 1 – 1 correspondence with the edges. In terms of these generators the fundamental group is not free. The relations can be used to set to one any generator corresponding to an edge connecting distinct points. Thus, for each such edge, we can define a contraction of the graph, which is a map sending it to another graph with the open edge removed and the two vertices at the end of the edge identified, see fig. 10. Under this map the fundamental group does not change [15]. We can continue this contraction process until the graph is mapped to a graph with one vertex and all edges incident on that vertex. We will call such a graph a *flower*. Its fundamental group is a free group on g generators. In fig. 11 we have drawn an example. Suppose c in (4.1) runs from 0 to R_I . Choose a region, say the one labelled 0, which we call the outside region, and the remainder are called interior regions. A convenient set of generators is the set of *oriented boundaries of the interior regions* ($W_c, c = 1, \dots, R_I$) which we call the *region paths*. The boundary of the outside region is not independent (proof in sec. 7). The contraction procedure allows a simple way to write the Wilson loop in terms of independent generators.

Step1: Choose some set of edges to be contracted, which allows us to map the Wilson graph to a flower. Then write the remaining edges in terms of the oriented region paths. Write each Wilson loop in terms of the chosen generators. Corresponding to this word in the fundamental group, draw a closed strand, joining a sequence of generators. Label the strand by an integer $n(\vec{k}_\Gamma)$ called its multiplicity.

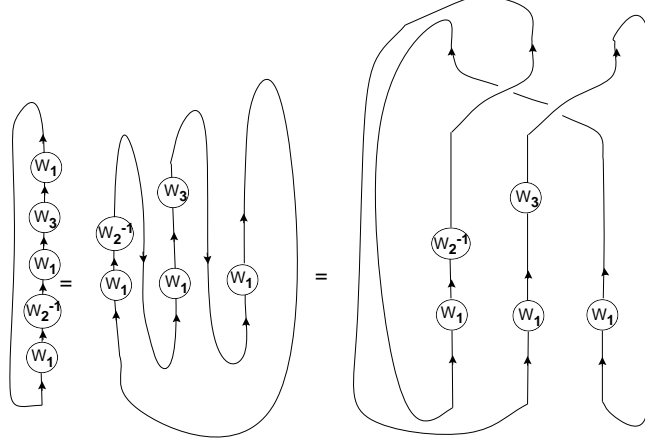


Fig. 12: Deforming a strand carrying generators of the fundamental group.

Step 2 : Choose an ordering of the generators. Set the array vertically with the first generator at the bottom. If a generator occurs more than once, then deform the strand to obtain an ordered set of generators together with some cyclic permutation, see fig. 11.

Step 3 : Repeat the procedure for all the Wilson loops and the inverse of the oriented boundary of the outside region and arrange them so that any given generator occurs at the same level in all strands. For the boundary of the outside region the label on the strand is equal to some integer n_0 which is summed over. Insert at the bottom of this strand the factor $F_0(n_0) = F(G_0, A_0, b = 1, n_0)$ the F factor for the outside region, its explicit form is given in (3.6). The first entry on the strand corresponding to a Wilson Loop is $\frac{1}{n(\vec{k}_\Gamma)!} \sum_{\sigma_\Gamma \in S_{n(\vec{k}_\Gamma)}} \sigma_\Gamma$. The strands are placed in some arbitrarily chosen order from left to right. At the end of this step, the central part of the diagram contains upward directed strands incident on W 's and the top and bottom of these strands are tied as in fig. 12.

Comments:

- a) To simplify the diagram it may be convenient to change the expressions of the Wilson loops independently to others in the same conjugacy class of the fundamental group, by conjugating with some generator.
- b) It is convenient to remove redundant expressions like a generator followed by its inverse.
- c) It follows easily by inspection of the flower (see fig. 11) , that the oriented boundary of the outside region can be written as a product of the inverse of the all the region paths in some order, each region path occuring once.

Starting with this diagram we will replace the generators of the fundamental group of the graph with sums over permutations acting on a set of numbers, to get a diagram generalising fig. 1, fig. 2, fig. 9, and fig. 5. All permutations will act on some subset of the integers ranging from 1 to the sum of all the multiplicities of the strands appearing in the diagram. A pair of strands with multiplicities m_1 on the left and m_2 to the right incident on a generator W_c is equivalent to a single strand of multiplicity $m_1 + m_2$ incident on W_c . The combined strand carries a natural action of S_{m_1} on the first m_1 strands, of S_{m_2} on the second set of m_2 strands, and of $S_{m_1+m_2}$ on the combined strand.

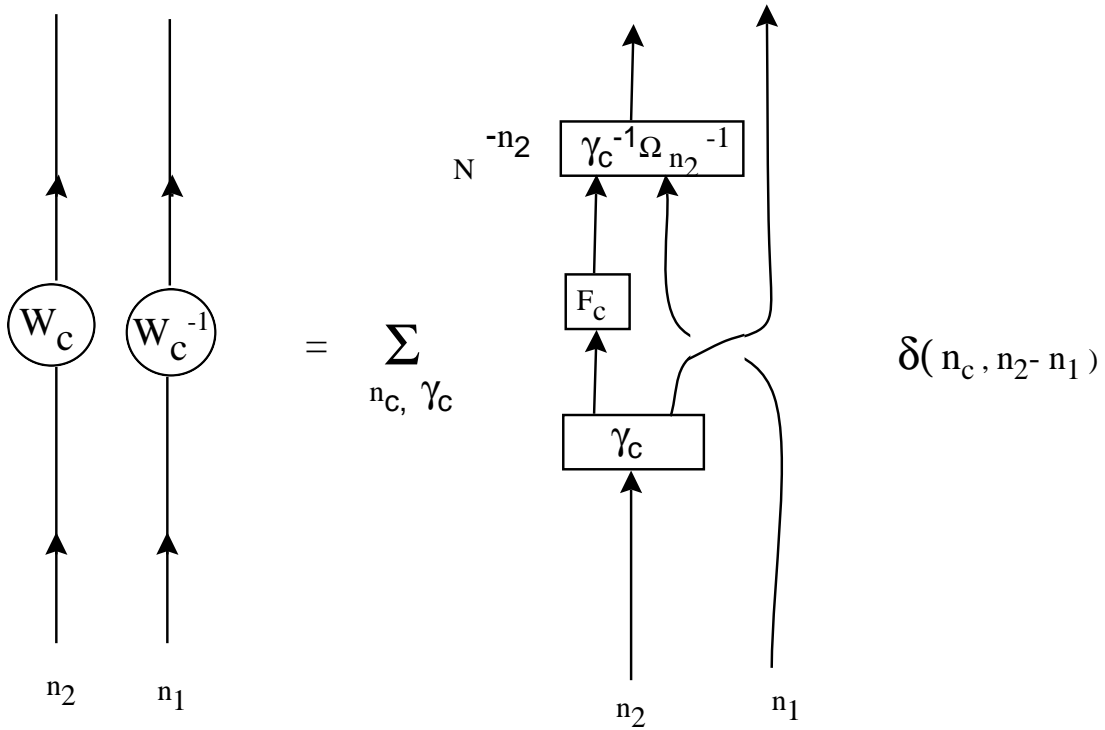


Fig. 13: The basic weight for the delta function

Focusing on the occurrences of a given generator W_c and its inverse, the diagram looks like the left hand side of fig. 13. We have used the usual shorthand of combining all the strands incident on W_c (or W_c^{-1}) into one strand.

Step 4: We will replace this by a sum over permutations acting on the labels carried by the strands as in the RHS of fig. 13. Because of the delta function which imposes $n_2 = n_c + n_1$, we have used the isomorphism between a strand of multiplicity n_2 and a pair

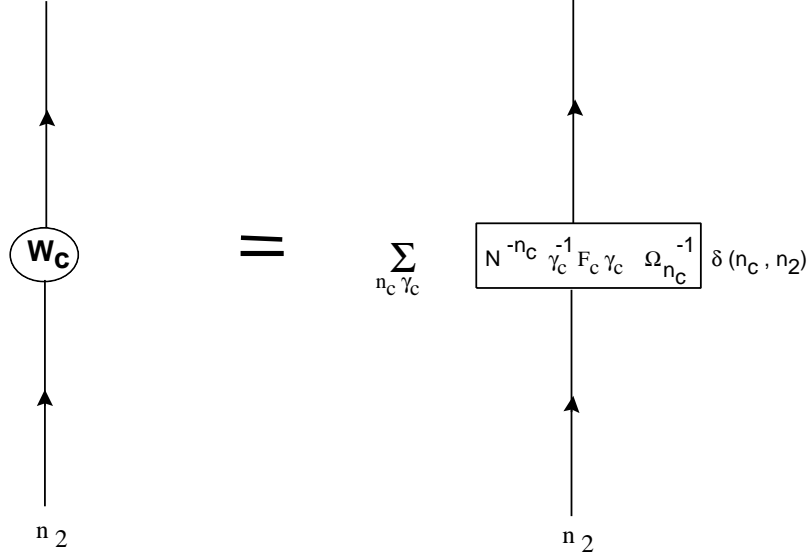


Fig. 14: Basic weight: simple case

of strands of multiplicities n_c and n_1 . The choice of letting the F_c act on the first n_c as opposed to the last say is done for convenience, and it does not change the result because of the sum over γ_c . In case there are only incidences of W_c the vertex simplifies to the one in fig. 14.

Step 5: At the top of the diagram, we place a factor $N^n \Omega_n$ where n is the total number of strands going upward counted with multiplicity, and we replace the solid lines joining top to bottom by dotted lines. This is the delta function. It is always a sum over homomorphisms from fundamental group of $\Sigma_T - \{\text{points}\}$ into symmetric groups, with certain restrictions on the allowed permutations which are in the diagram.

Comment:

In the general case of Wilson loops in a closed manifold, the exact answer is constructed by starting with delta functions of for manifolds with boundary obtained by cutting along the Wilson loops. These boundary permutations also enter a complicated delta function of the kind we discussed, with embeddings of symmetric groups into a large one, determined by the Wilson loops. By solving for the boundary permutations we can combine into a single delta function containing F factors (see appendix). When we have Wilson loops in a manifold with boundary, the single delta function will contain F factors and permutations

associated with the real boundaries (not those associated with cutting along the Wilson loop).

We will now describe the derivation of the rules from the group integrals and outline a proof that expectation values for chiral intersecting Wilson averages compute the Euler character of Hurwitz-Wilson space. We will illustrate this in a simple example.

7. Derivation of algorithm

We will use the exact results on Wilson averages in terms of integrals over the gauge group described in section 4.

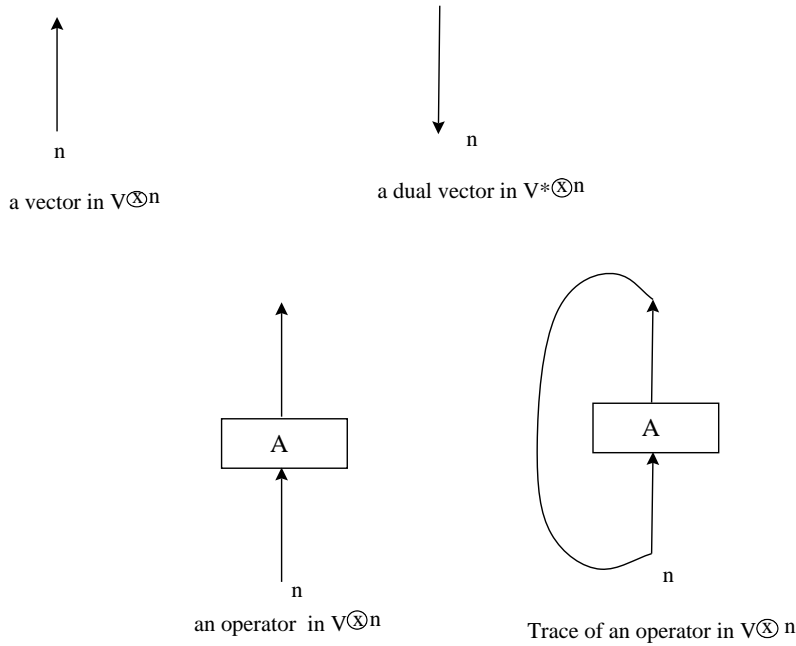


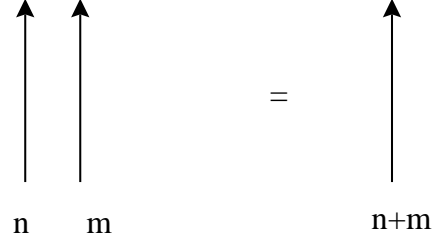
Fig. 15: vectors and operators.

7.1. From group integrals to braid diagrams

Three simple ingredients go into the derivation of these rules. First we use a basic relation between gauge invariance and fundamental groups.

Second we make extensive use of a diagrammatic approach to linear algebra in tensor spaces (more generally to Braided Tensor Categories) which may be familiar from many contexts , and has been useful before in algebraic constructions of topological invariants, e.g knot and 3-manifold invariants, and for proving properties of RCFT. [16,17,18]

Finally we use a few integrals which can be derived from Schur-Weyl duality.



a vector in $V^{\otimes n} \times V^{\otimes m} \cong V^{\otimes n+m}$

Fig. 16: vectors in tensor space: a basic isomorphism

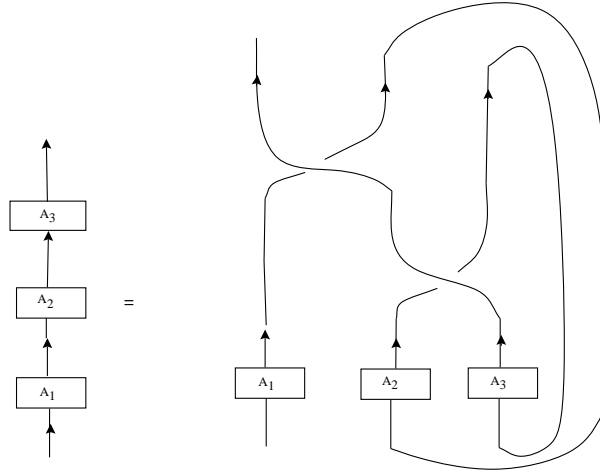


Fig. 17: Linearising Group Multiplication in tensor space.

The basic diagrammatic presentation of vectors, endomorphisms and traces is shown in fig. 15. A basic isomorphism between tensor spaces is shown in fig. 16. A very useful identity is shown in fig. 17. Writing it out, using summation convention for repeated indices, we have

$$\begin{aligned}
 RHS &= (1 \otimes tr \otimes tr) P_{(123)} A_1 \otimes A_2 \otimes A_3 |e_{i_1} \rangle \otimes |e_{i_2} \rangle \otimes |e_{i_3} \rangle \\
 &= (1 \otimes tr \otimes tr) P_{(123)} (A_1)_{i_1}^{j_1} (A_2)_{i_2}^{j_2} (A_3)_{i_3}^{j_3} |e_{j_1} \rangle \otimes |e_{j_2} \rangle \otimes |e_{j_3} \rangle \\
 &= (1 \otimes tr \otimes tr) (A_1)_{i_1}^{j_1} (A_2)_{i_2}^{j_2} (A_3)_{i_3}^{j_3} |e_{j_3} \rangle \otimes |e_{j_1} \rangle \otimes |e_{j_2} \rangle \\
 &= 1 \otimes \langle e^{i_2} | \otimes \langle e^{i_3} | (A_1)_{i_1}^{j_1} (A_2)_{i_2}^{j_2} (A_3)_{i_3}^{j_3} |e_{j_3} \rangle \otimes |e_{j_1} \rangle \otimes |e_{j_2} \rangle \\
 &= (A_1)_{i_1}^{i_2} (A_2)_{i_2}^{i_3} (A_3)_{i_3}^{j_3} |e_{j_3} \rangle \\
 &= (A_3 A_2 A_1)_{i_1}^{j_3} |e_{j_3} \rangle = LHS.
 \end{aligned} \tag{7.1}$$

The identity has an obvious generalisation to a product of n elements:

$$(1 \otimes tr \otimes \cdots tr) P_{(12 \dots n)} (A_1 \otimes A_2 \cdots A_n) = (A_n \cdots A_2 A_1). \quad (7.2)$$

We perform for each $Z_c(U_1^{(c)}, U_2^{(c)}, \dots, U_{b_c}^{(c)})$ the chiral expansion, replacing the sum over all representations by a double sum, over the number of boxes n and the set of Young diagrams with n boxes. This will yield

$$Z_c(U_1^{(c)}, U_2^{(c)}, \dots, U_{b_c}^{(c)}) = \sum_{n_c=0}^{\infty} \frac{1}{n_c!} \delta \left(F(A_c, G_c, b_c, n_c) u_1^{-1} \cdots u_{b_c}^{-1} \right) \Upsilon_{u_1}(U_1^{(c)}) \cdots \Upsilon_{u_{b_c}}(U_{b_c}^{(c)}). \quad (7.3)$$

The F factor is obtained from (3.6). The loop functions will be integrated over. Let us now restrict to the case where each region Σ_T^c has one boundary. This will bring out the key features which make the intersecting case different from the non-intersecting case. In this case the delta function will set F_c equal to u_c , and the u_c enters a braid diagram, so we can do the sum over u_c producing F_c in the braid diagram.

So we now have a product

$$< W > = \int \prod_c \sum_{n_c} \frac{1}{n_c!} \delta_{n_c}(F_c u_c^{-1}) \Upsilon_{u_c}(V_c) \prod_{\Gamma} \sum_{\sigma_{\Gamma} \in [\vec{k}_{\Gamma}]} \frac{1}{n(\vec{k}_{\Gamma})!} \Upsilon_{\sigma_{\Gamma}}(U_{\Gamma}^{\dagger}) \quad (7.4)$$

The integral is over all the edge variables. The V_c are expressed in terms of the edge variables.

Now the first observation is that following a standard argument in lattice gauge theory we can set to 1 group variables associated with edges connecting distinct points. Recall that a gauge transformation in lattice gauge theory can be specified by giving a group variable g_i for the i 'th vertex. The holonomy U_{ij} is transformed to $g_i U_{ij} g_j^{-1}$. Consider an edge joining two distinct points, k and l with holonomy U_{kl} . Let the group variable g_l be related to g_k by $g_l = g_k U_{kl}$. This gauge transformation sets to 1 the variable U_{kl} . This specifies a conjugation for the holonomies along the remaining edges which can be absorbed into the Haar measures for these variables. We are left then with an integral over U_{kl} where the integrand is independent of U_{kl} . The integral gives 1 (the Haar measure is normalised such that the group volume is 1).

This shows that the integral is unchanged if such an edge is contracted until k and l become a single point. If this deformation is done while keeping the areas of all the

regions fixed, the Wilson average is unchanged, e.g the Wilson loops in fig. 10 have the same expectation value if the areas are left unchanged in the deformation. Note that as the contraction is done the *Euler character of the Wilson graph is not changed*. The contraction procedure can be repeated until the only variables left are closed loop variables. The process of contracting the edges does not change the fundamental group of the graph. In fact this is used in [15] to show that the fundamental group of a graph is a free group.

Having set to 1 some set of edges such that the reduced graph is a flower, we find it convenient to choose one region which we call the outside region, Σ_T^0 , and use as independent variables, the holonomies V_c around the R_I interior regions. The choice of these variables is convenient for an intuitively clear geometrical interpretation, but other choices can be made and have to be made, e.g for higher dimensional models. In the case of interest here, let us prove that our chosen variables form a complete set. This may be seen by computing the Euler character of the target in two ways:

$$\begin{aligned}\chi(\Sigma_T) &= \chi(\text{graph}) + \sum_{c=0}^{R_I} (1 - 2h_c) \\ &= 2 - \sum_{c=0}^{R_I} (2h_c).\end{aligned}\tag{7.5}$$

Now use the fact that $\chi(\text{graph}) = 1 - g$ to find that $R_I = g$. The holonomy around the outside, can be written $\prod_c V_c^\dagger$ in some order. The Wilson averages are also expressed in terms of the V_c 's. Using the conventions of fig. 15 we can write the $\Upsilon_{u_0}(V_0) = \text{tr}_{n_0}(u_0 V_0)$ as a vertical strand containing u_0 at the bottom and a sequence of interior V_c^\dagger 's, and with the upper end of the strand tied back to the lower end. We do the same thing with the Wilson loops. We arrange the diagram such that all the V_c 's and V_c^\dagger 's for a given c occur at the same level. To arrange this we may need to use the fact from linear algebra (7.2), which has the diagrammatic interpretation fig. 17. So we have accounted for steps 1 to 3 of the algorithm in section 7. At the end of this we have a sequence of operators in tensor space, consisting of permutations, and integrals of the form $\int dV_c \Upsilon_{u_c}(V_c) \rho_{n_2}(V_c^\dagger) \rho_{n_1}(V_c)$.

$$\int \begin{array}{c} \uparrow \\ U \\ \uparrow \\ n_1 \end{array} \begin{array}{c} \uparrow \\ U^\dagger \\ \uparrow \\ n_2 \end{array} = \delta_{n_1, n_2} \sum_{\gamma} \begin{array}{c} \uparrow \quad \uparrow \\ \gamma \quad \gamma^{-1} \Omega_{n_1}^{-1} N^{-n_1} \end{array}$$

Fig. 18: Basic integral

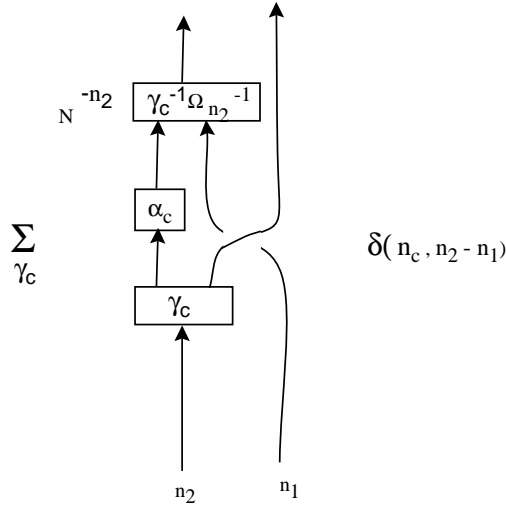


Fig. 19: Integral derived from basic integral .

This is derived by using the integral $\int dU \rho_{n_2}(U^\dagger) \rho_{n_1}(U)$. For large $n_1, n_2 \leq N$, it is expressed in terms of Ω factors in [1]. Then the integral is proportional to δ_{n_1, n_2} , and is expressed in diagrammatic notation in fig. 18. The result for $\int dV_c \Upsilon_{u_c}(V_c) \rho_{n_2}(V_c^\dagger) \rho_{n_1}(V_c)$ an operator on $V^{\otimes n_2} \otimes V^{\otimes n_1}$ is shown in diagrammatic notation in fig. 19. Note we have used the isomorphism $V^{\otimes(n_c+n_1)} \cong V^{\otimes n_c} \otimes V^{\otimes n_1}$. Now u_c also appears in $\delta(F_c u_c^{-1})$, so after doing the sum over u_c , we recover step 4 of section 7. After doing all the integrals using this formula we have a trace in tensor space of certain permutations. This is converted to a delta function using (2.6). This is step 5 of section 7.

Comment: In the general case we have delta functions of the type we get for manifolds with boundary from the Z_c factor as in (7.3). The permutations entering here also enter more complicated delta functions. The latter come from doing group integrals. All the

integrals needed can be expressed in diagrammatic form using the integrals presented in this section. Combining the delta functions into a single one proceeds by simple operations on braid diagrams, e.g connected sums (see appendix).

8. Braid Diagrams and Branched covers

To relate the large N expansion to branched covers, we will show how to construct branched covers from the data in the delta function, using cutting and pasting techniques of Hurwitz. We will sketch briefly the converse : how the symmetric group data can be extracted from the covers.

We will then explain how all the key features of the general construction can be understood in terms of Euler characters of Hurwitz -Wilson spaces. This will involve showing that the Gross-Taylor rule, and a generalisation, has a simple interpretation in terms of Euler characters of Hurwitz-Wilson spaces.

The result of applying the algorithm of section 6 to an example of intersecting Wilson loops will be written down in section 10. Its interpretation in terms of branched covers and Euler characters of spaces of branched covers will be demonstrated.

8.1. From Braid diagrams to Branched covers

The braid diagram is just a more elaborate version of fig. 1, with the allowed permutations having some special structure. Exploiting this observation, we see that the easiest way to construct the covers starting from the braid diagram is to start with a branched cover of constant degree. Then we cut along the boundaries of the various regions Σ_T^c to obtain the right degrees (as dictated by the powers of $1/N$, the string coupling constant), in the various regions. The degrees are easily read off from the braid diagram by inspecting the number of strands that the F_c factor acts on. They also follow from inspection of the group integral for each edge, which imposes some selection rules on the difference in degree between regions on the left and right of the edge [1]. We will illustrate such a construction which starts with a branched cover of constant degree using usual techniques of construction of branched covers and makes cuts as instructed by the braid diagram to produce a cover satisfying the condition (4.4).

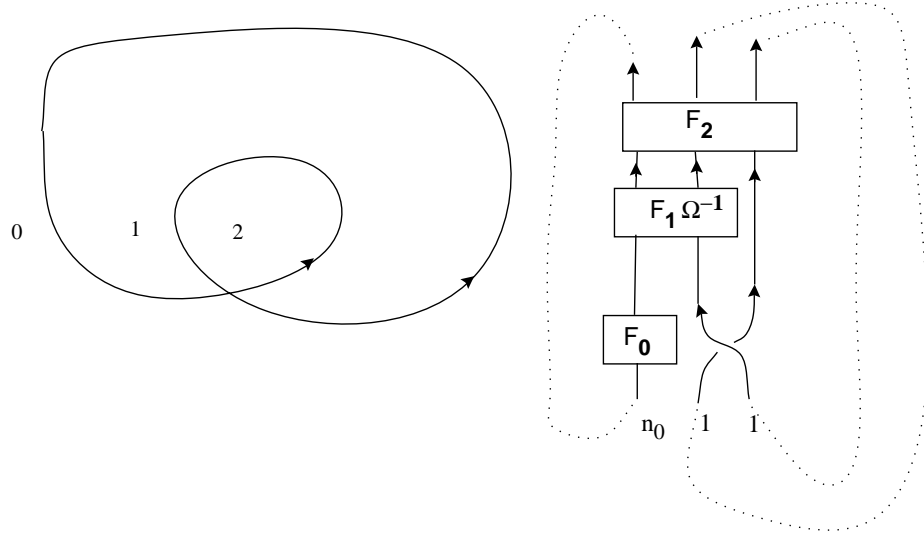


Fig. 20: a Wilson loop and its braid diagram

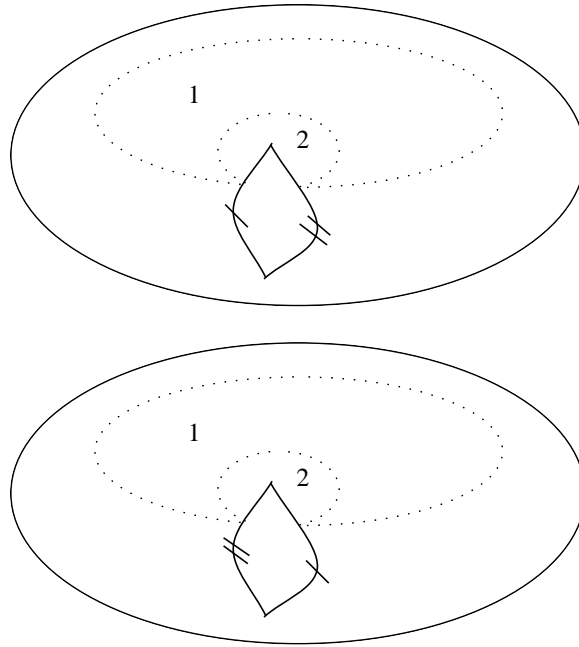


Fig. 21: The cut and paste construction.

Consider the example Wilson loop shown in fig. 20. We have drawn a sketch of the braid diagram obtained by following the rules of section 6 . For simplicity we are considering a Wilson loop in fundamental representation, but the delta function keeps the same form in the general case. We have also cancelled the conjugating γ factors (we can do this since they commute with the F 's in this case) which are unnecessary since we are not

concerned with the detailed counting at this point, but rather in construction techniques for branched covers. One solution to the delta function is obtained by setting $F_1 = F_0 = 1$, and F_2 a transposition acting on the two strands coming from the Wilson loop. The extra winding present from the construction of the braid diagram, is like a simple branch point, but does not carry the usual factor of $1/N$ for simple branch points. Opting for the simplest cut and paste construction of covers with two simple branch points, we make two slits joining the branchpoints and then identify the edges as indicated in fig. 21. Then we get the correct degree (namely 1 for region 1 and 2 for region 2, and 0 for outside region) by cutting both top and bottom sheets along the larger dotted circle and dropping the part covering the outside, and only the top sheet along the smaller dotted circle throwing the part covering region 1. The fact that the simple branch point which gets associated with the outside doesn't have the usual $1/N$ is that this permutation acts on sheets that are eventually removed; its role is to produce the correct winding of the Wilson loop. This basic construction generalises to arbitrary braid diagrams and shows that, in the chiral theory, **the only singularities we need are branch point singularities**.

The permutations in F_c are associated with branch points and handles in region Σ_T^c , as viewed from a basepoint in Σ_T^c . The γ_c instructs us on how to tie the covers of the separate regions along Γ . There may also be extra branch points that have to be inserted in region c , but which permute sheets that will be cut out in the final step. We saw this already in the non-intersecting case, and in the example above. Extra branch points are needed in sheets that will be cut out because they produce the correct monodromy along the Wilson lines for the maps from the worldsheet boundaries to the Wilson graph.

Remark: Relation between Hurwitz-Wilson spaces and CLOSED strings.

In fact for a non self-intersecting Wilson loop which has on its right a surface with G handles, an insertion of $N^{|\vec{k}_\Gamma| - 2Gn(\vec{k}_\Gamma)}$ times the usual insertion would count covers where one does not need to cut along that Wilson loop. For self intersecting loops the renormalisation needed would also depend on the windings of the Wilson loop and can be read off from the delta function constructed according to the rules above. With these renormalisations, Wilson averages count Euler characters of subspaces of ordinary Hurwitz spaces for closed worldsheets. For example, for a general Wilson loop on the sphere the renormalisation needed is $N^{|\vec{k}_\Gamma|}$. For higher genus targets different renormalisations may be needed according to different ways of embedding Hurwitz-Wilson spaces inside Hurwitz spaces. These correspond to different choices that can be made in constructing the delta functions. These choices appear, on the one hand, in how one writes the integrals, and geometrically in how one chooses generators of the fundamental groups, and basepoints, etc. to describe the covers in Hurwitz-Wilson spaces.

8.2. From branched covers to Braid diagrams

Choose a region which we call the outside region and a basepoint in it. Choose one basepoint on the edge and one in the interior of each region cut out by the Wilson loops. Choose a set of paths each homotopic to a path around c 'th region traversed in a direction compatible with the orientation of that region. If the boundary of the c 'th region has a branch point, deform the path to the right of the Wilson loop.

Suppose the degree of the map is n_0 on the outside. Label from 1 to n_0 the inverse images of the basepoint, and draw points corresponding to these in a row which will be the base of the braid diagram. Complete the cover as discussed before. There may be more than one prescription for completing the cover, these correspond to different ways of writing the braid diagram, which are related by identities in tensor space.

Permutations in the F_c factors will be picked up, by lifting paths based in the respective regions in the usual way as for manifolds with boundary and for non-intersecting Wilson loops. The conjugating permutations γ_c will be read off by lifting paths connecting the basepoints in the region to basepoints on the Wilson loop. We will see this in detail in an example in the next subsection.

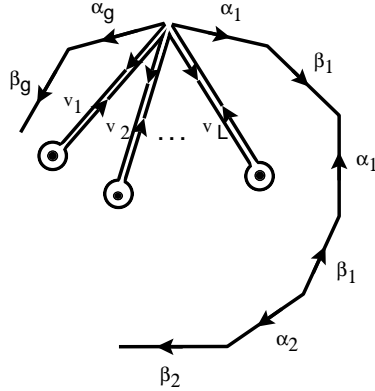


Fig. 22: Ordered set of generators

Remark: Ordering the generators.

The fact that the braid diagram contains all regions in a chosen order from down to up corresponds to the fact that the product of permutations produced in all regions is 1. This just follows from the 1 relation on the generators of the fundamental group of $\pi_1(\Sigma_T - \text{branch points})$. It is clear geometrically that we should be able to construct

the braid diagram by choosing any ordering of the regions. This ordering corresponds to the fact that the relation satisfied by the generators of the fundamental group of a Riemann surface with punctures are expressed by choosing some ordering of the generators. Geometrically, having made a choice of representatives of the non trivial classes of the fundamental group there is a definite cyclic order in which we have to take the product of these paths to get a path that spans a 2-cell and is therefore trivial, see fig. 22. That the ordering of the regions in the braid diagram can be changed arbitrarily can be recovered as a consequence of Weyl duality and cyclicity property of traces.

8.3. *Equivalences and Automorphisms*

A combinatoric definition of equivalence is an action of the symmetric groups involved which preserves the delta function. We can read off from the braid diagram an action of the symmetric groups which leaves the delta function invariant, and indicate the relation to an automorphism of the cover constructed from the braid diagram. To give an equivalent braid diagram we specify permutations x_c for each component, which act by conjugation on all the permutations in the F factor. These correspond to relabelling the points in the inverse image of the basepoint in the regions Σ_T^c . We also specify permutations x_Γ associated with the Wilson loops for the basepoints on the boundary of each region. Let β_c denote the winding that occurs when the vertex contains both positive and negative powers of a generator fig. 13. The action on the γ_c and β_c is determined by requiring that the product of the

$$\gamma_c^{-1} F_c \beta_c \gamma_c,$$

is conjugated by the product of x_0 and x_Γ 's for the strands acted on by the γ_c , F_c and β_c . Let us call x_a the combination that relabels the first two strands in fig. 13, and x_b the one that relabels the last one. We find that the action

$$\begin{aligned} \gamma_c &\rightarrow (x_c.1.1)\gamma_c(x_a.1)^{-1} \\ F_c &\rightarrow (x_c.1.1)F_c(x_c.1.1)^{-1} \\ \beta_c &\rightarrow (1.1.x_b)\beta_c(1.1.x_b)^{-1} \end{aligned} \tag{8.1}$$

guarantees the conjugation. These relabellings correspond to restrictions of the map ϕ to the various basepoints y_c in the regions Σ_T^c and those on the Wilson graph, used in relating maps to the homomorphism into permutation groups. The equation (8.1) does not lead to a unique way of setting up symmetric group actions which preserve the delta

function. Different choices should correspond to different ways of setting up the description and counting of the covers.

Once we know that equivalence classes of maps are in $1 - 1$ correspondence with equivalence classes of homomorphisms under the combinatoric equivalence just defined, it is clear that the centraliser subgroup of an equivalence class of homomorphisms is isomorphic to the group of automorphisms of the branched cover. Counting the homomorphisms represented in the braid diagram with weight equal to the orders of the permutation groups involved is the same as counting equivalence classes of homomorphisms with weight equal to the inverse order of the centraliser subgroup. This shows that the symmetric group data in the braid diagram counts equivalence classes of maps with weight equal to the inverse order of the automorphism group.

9. Euler Characters of Hurwitz-Wilson spaces

For the partition functions we saw that the power of Ω factors is equal to the Euler character of the target space, and for maps of degree n the Ω factor has degree n . After expanding the Ω factors this led to the result that the number of branched covers counted with inverse order of automorphism group, was weighted by the Euler character of the configuration space for motion of the branch points on the target. This was, for fixed degree, branching number and fixed number of branch points, the Euler character of Hurwitz space, a discrete bundle over configuration space. Here the base space of the bundle will be the product of configuration spaces for the separate regions labelled by c and for the graph defined by the Wilson loops. The number of Ω factors appropriate for each region appears in the F factors. Then there are inverse omega factors for each generator of π_1 and an Ω factor. We prove for arbitrary Wilson loops

Theorem 9.1 The net number of Ω factors (outside the F factors) is equal to the Euler character of the Wilson graph.

Proof

This follows from the fact that the contraction procedure does not change the Euler character, since each contraction reduces the number of edges by 1 and the number of vertices by 1. The Euler character of the reduced graph is clearly the $1 - g$ where g is the number of generators of π_1 . In our integration scheme we choose these g generators to be the interior region paths. Each integration gives an inverse omega factor Ω^{-1} , and going from traces to delta functions using (2.6) we get an Ω factor. ♠

Remark : This property has a generalisation beyond Wilson loops in two dimensions, and motivates a conjecture on the relation between the Euler characters of an appropriate space of branched covers and higher dimensional Lattice gauge theory. We return to this briefly in the final section.

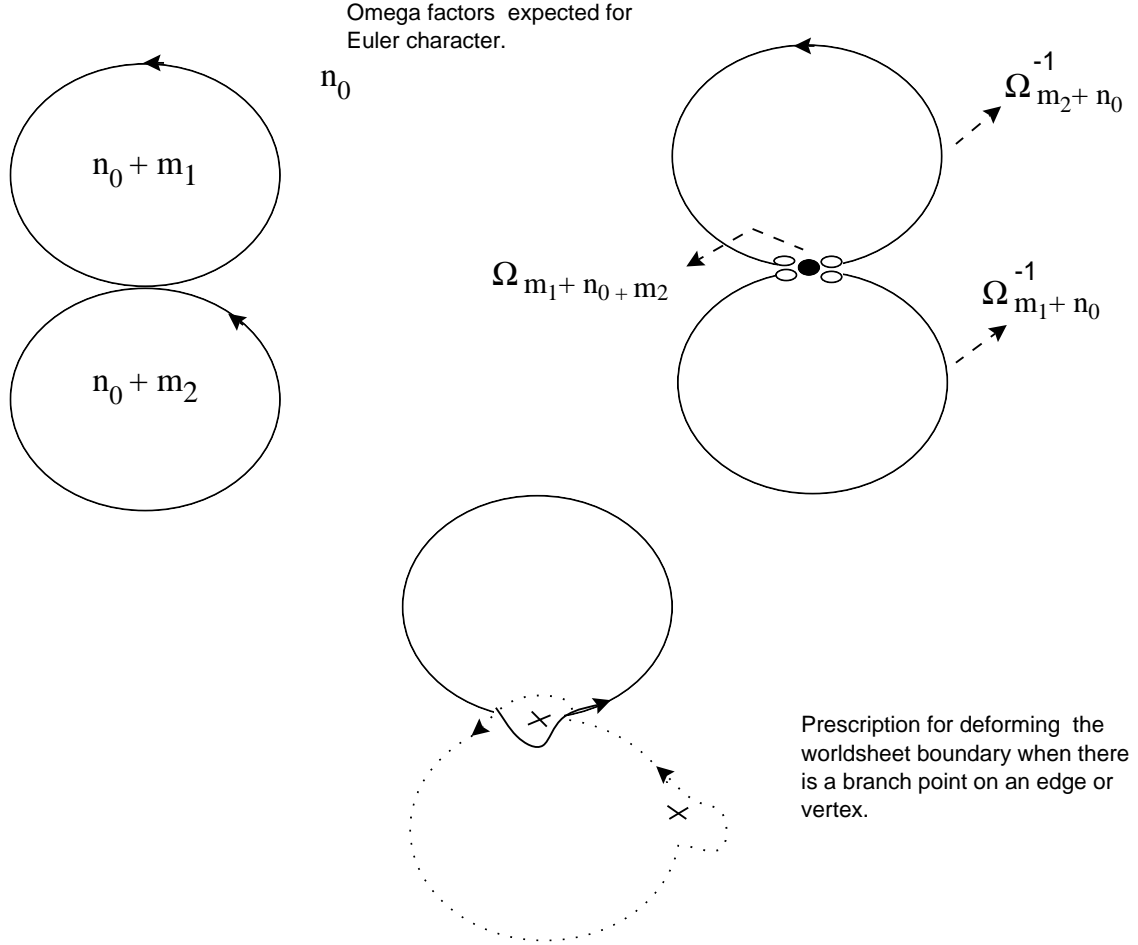


Fig. 23: Omega factors and branch points on Wilson graph.

9.1. Detailed placing of Omega factors, Euler characters and the Gross Taylor prescription.

Having discussed the net number of Omega factors in complete generality, we now turn to the detailed nature of the Omega factors which appear, in particular, the degree d of Ω_d and the power with which it appears. We have a space of branched covers where the branch points are allowed to be anywhere on the Wilson graph and an important point is that the *degree of the map is not constant over the graph*. To calculate the Euler character of such a space of branched covers, we should decompose the Wilson graph into edges,

vertices and for convenience we will allow circles, such that the degree of the map restricted to any such component is constant.

Distributing Omega factors :

We then assign to each component a factor Ω_d^χ where d is the degree of the map restricted to that component and χ is the Euler character of that component.

This predicts which Ω factors appear in the delta function. It is equivalent to the Gross Taylor rule when the latter is directly applicable (transversal double intersections) and generalises it to arbitrary Wilson loops. The Gross Taylor approach instructs us to perturb the inverse Omega factor from each edge into the side to its left, which predicts the degree of the Omega factor. For a vertex where two edges intersect transversally, it tells us to perturb the Ω factor to the left of both edges. Again this predicts the same degree as the above. Our interpretation however is different. We allow the *branch points to lie on the graph*, and give a prescription for *deforming the paths* along which the monodromies are measured.

When the omega factors are expanded out they produce branch points which are interpreted to lie on the graph. Reconstructing the delta function from the map proceeds as before. The monodromies are well defined using the prescription of deforming the image of the worldsheet boundary away from the branch point, to the right of the oriented Wilson loop. When we restrict the delta function to the strands corresponding to the Wilson loop, we are taking a path which is the image of the deformed worldsheet boundary, i.e it is deformed to the right of the branch point. fig. 23 illustrates our prescriptions with a graph that has a tangential intersection.

We comment on the distribution of Omega factors that comes from the rules of integration we described. It is most clearly understood in terms of covering spaces of the reduced Wilson loop. The omega factor is naturally associated with the vertex of the reduced graph. The inverse omega factors are associated with edges according to the number of sheets they act on. For reduced graph and unreduced graph, the rule based on Euler characters of Hurwitz spaces, gives different distributions of Omega factors. These are expected to be related by identities in the algebra $Z(S_\infty) \times \mathbb{R}(1/N)$, or equivalently in the group algebra of arbitrarily large symmetric groups tensored with power series in $1/N$. Typically the identities involve equation 11.3 and its generalisations.

The final step in the proof of Theorem 9.2 proceeds as before.

Theorem 9.2 The Chiral Wilson average counts Euler characters of Hurwitz-Wilson spaces.

We expand the Ω factors. The F_c -factors contain $2 - 2G_c - 1$ omega factors so these generate Euler characters of configurations of points in the respective regions Σ_T^c . The extra Omega factors associated with the Wilson graph generate Euler characters of configuration spaces of points on the graph. So each term in the Wilson average is a product of Euler characters of configuration spaces times discrete data counting, with inverse automorphisms, Hurwitz Wilson branched covers for fixed branch locus. This completes the proof.

10. Example

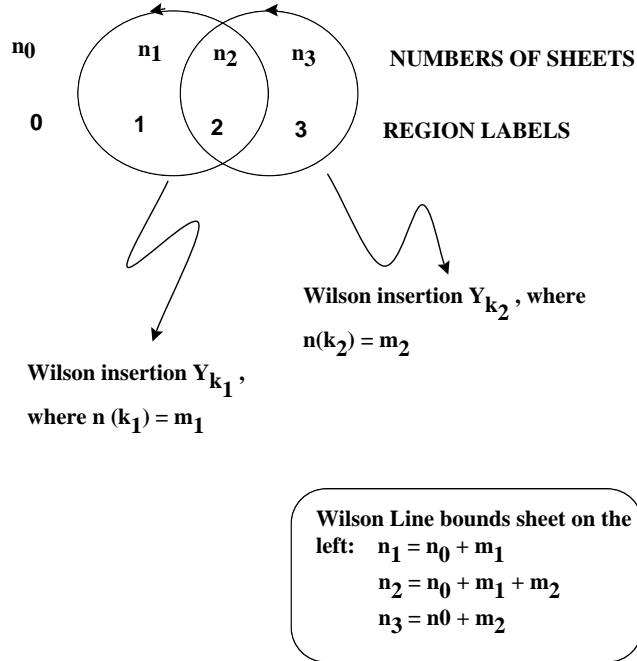


Fig. 24: A pair of Borromean rings

We discuss here a simple example (fig. 24) which illustrates how the chiral large N expansion generalises to intersecting Wilson loops, and admits an interpretation as a generating function for Euler characters of Hurwitz-Wilson spaces. We consider a pair of Wilson loops which intersect twice. The Wilson loops 1 and 2 are labelled by the vectors \vec{k}_1 and \vec{k}_2 , with $n(\vec{k}_i) = \sum_j j k_i^{(j)} = m_i$. The answer is illustrated diagrammatically in fig. 25. The sums over n_i are restricted by the conditions written in fig. 24. The permutations σ_i ($i = 1, 2$) are summed over the conjugacy classes specified by \vec{k}_i in S_{m_i} .

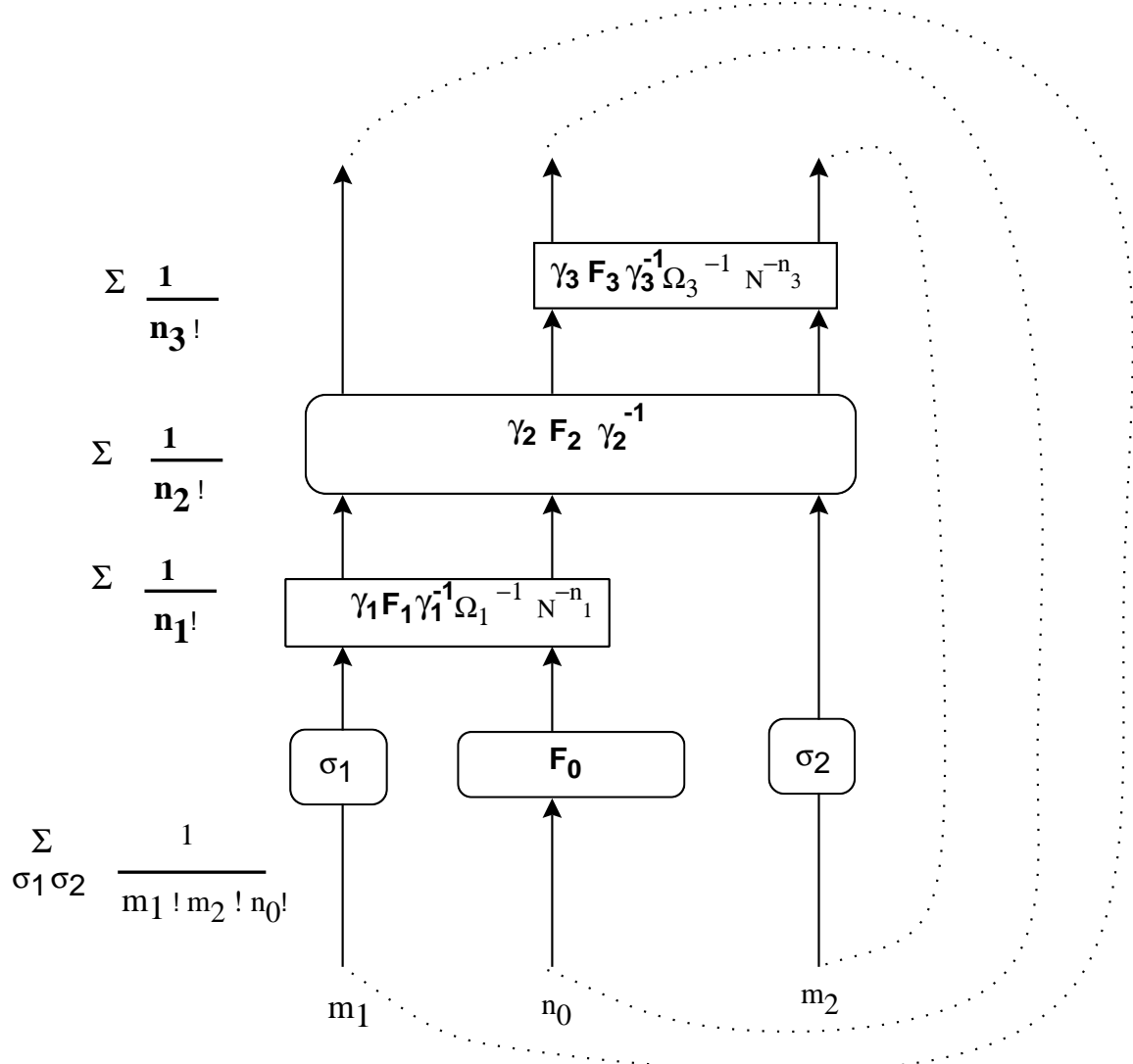


Fig. 25: Braid diagram for Borromean rings

10.1. From Braid diagram to maps, and automorphisms

The discussion of how to go from braid diagram to maps has already been given in complete generality. We just state the main points as applied to this example. Start with a covering of constant degree $n_0 + m_1 + m_2$ by the same techniques that were used for covering surfaces counted by the partition function, and cut out a number of sheets to the right of each Wilson loop at the end. The only difference here is that there are specified monodromies along the Wilson loops, which restricts the kind of branch points that are allowed. Branch points coming from expanding the F'_c s are clearly to be placed in the respective regions c . In the example shown we also need to add branch points giving

monodromies σ_1 and σ_2 on the m_1 and m_2 sheets outside. These sheets are going to be cut out from the outside along the Wilson loops 1 and 2 respectively but they guarantee that the right monodromy is recovered from paths along the Wilson loops.

We discuss here in detail the issue of equivalences and automorphisms.

In the example, the n_0 points at the base of the braid diagram can be relabelled according to permutations $x_{\Gamma_1}.x_0.x_{\Gamma_2} \in S_{m_1} \times S_{n_0} \times S_{m_2}$, to give maps related by a homeomorphism ϕ . The basepoints in the Σ_T^c can be relabelled by permutations x_c . x_c acts on the permutations in F_c by conjugation, which leads to

$$F_c \rightarrow x_c F_c x_c^{-1}. \quad (10.1)$$

x_Γ acts on the permutations σ_Γ by conjugation. The action on the γ 's needed to leave the delta function invariant can be read off from the braid diagram. For example γ_1 is acted on the left by x_1 , and from the right by $(\sigma_1.x_0)^{-1}$. These relabellings correspond to restrictions of the map ϕ to the various basepoints used in going from the map to the homomorphism into permutation groups. Applying a theorem from the theory of branched covers [19], this shows that the data x_c, x_{Γ_i} is equivalent to a geometric equivalence ϕ . For ordinary branched covers the argument is reviewed in [13] and briefly in section 3 of [2].

10.2. From Maps to Braid diagrams

It follows immediately from conjecture 4.1, that the degrees of the maps in the various regions are related as shown in the diagram. The Wilson average contains a sum over n_0 , which is the degree of the map for the region outside. The cover may be completed by adding m_i sheets to the outside of Γ_i , which cover the outside, with just one branchpoint in the class specified by \vec{k}_i .

Let us ignore for a moment the omega factors outside the F_c . The F_c describe permutations associated with branch points and handles in region c . We can understand how a sequence of permutations satisfying the delta function can be obtained from a map of type described in section 8.5.1, *by restricting it, in turn, to the three sets of strands of multiplicity n_0 , m_1 and m_2 respectively*.

Choose a basepoint y_0 on the outside. Label the inverse images from 1 to n_0 , and correspondingly draw the n_0 middle points at the base of the braid diagram. Follow the lift of a path from the outside joining the basepoint outside to some point P_1 on Γ_1 . The

endpoints of the lifts will be points in the interior of the worldsheet. There will be m_1 extra points on the outside which lie on the boundary of the worldsheet. These can be mapped to m_1 points in the inverse image of y_0 for the *completed* cover. Repeat the procedure by choosing a basepoint P_2 on the second Wilson line. With the completed cover we have $n_0 + m_1 + m_2$ points in the inverse image of y_0 which correspond to points at the base of the braid diagram in direct analogy to the partition function.

Also choose basepoints in the interior of regions 1 through 3, and read off permutations around non-trivial cycles in these regions. These permutations enter the factors F_1 through F_3 . The permutations γ_c ($c = 1, 2, 3$) are obtained by following paths from regions c to the point y_0 . Using the conjugations all permutations are described with respect to one basepoint y_0 .

Now consider the lifts of curves which start from any of the n_0 points on the outside. Consider a product of paths around all the branch points and the appropriate commutators for the handles in region 0, 1, 2 and 3. It is homotopic to the trivial path. This is reflected in the braid diagram by the fact that the result of the windings of the n_0 strands produced successively by F_0 , F_1 , F_2 and F_3 is a trivial permutation. Restricting to the m_1 sheets, which only cover regions 1 and 2, we see that the image in $S_{n_0+m_1+m_2}$ of the path round region 1 times the image of the path round region 2 which is homotopic to the oriented path described by the Wilson loop Γ_1 is in the class of \vec{k}_1 , as in Conjecture 9.1. The same argument applies to Γ_2 which is homotopic to the product of paths around regions 2 and 3.

The same discussion goes through when we consider branch points coming from the extra Ω factors, by using the deformation of paths described in section 4.2 and 9.1.

10.3. Euler characters

In this example a decomposition of the graph satisfying the above conditions is shown in fig. 26. The degree of the map on the left edge is n_1 and on the right it is n_3 . This explains why the delta function contains $\Omega_{n_1}^{-1}$, $\Omega_{n_3}^{-1}$, $\Omega_{n_2}^0$. Proof that we have Euler character of Hurwitz-Wilson space proceeds as in section 9.

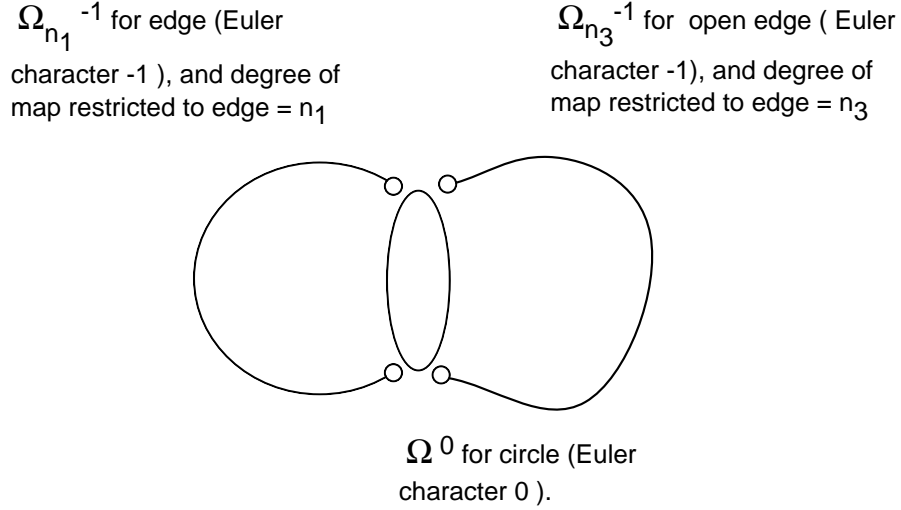


Fig. 26: Decomposing 2 intersecting circles into components where map has constant degree.

11. Chiral Loop Equations ²

In this section we use the diagrammatic formalism that we developed in the previous sections to prove that the Migdal-Makeenko loop equations are valid for Wilson loops in the chiral expansion ³.

The figure explains a proof of the Migdal-Makeenko equations for the chiral theory. These are differential equations giving the result of acting by a first order differential operator on the expectation value of Wilson loops (in the fundamental representation) with an intersection as in the top left of fig. 27 to the Wilson average with the intersection replaced by the top right of fig. 27. The differential operator is a combination of derivatives in the areas on different sides of the intersection.

Since the Wilson average is a sum over coverings of the target, such that the oriented worldsheet boundaries map to the oriented Wilson lines by orientation preserving maps, the degrees of the maps in regions 1 through 4 are related as in fig. 27. This corresponds in

² I thank G. Moore for collaboration on this section.

³ The observation that the Migdal-Makeenko Loop equations are valid for the chiral theory has been made independently by W. Taylor.

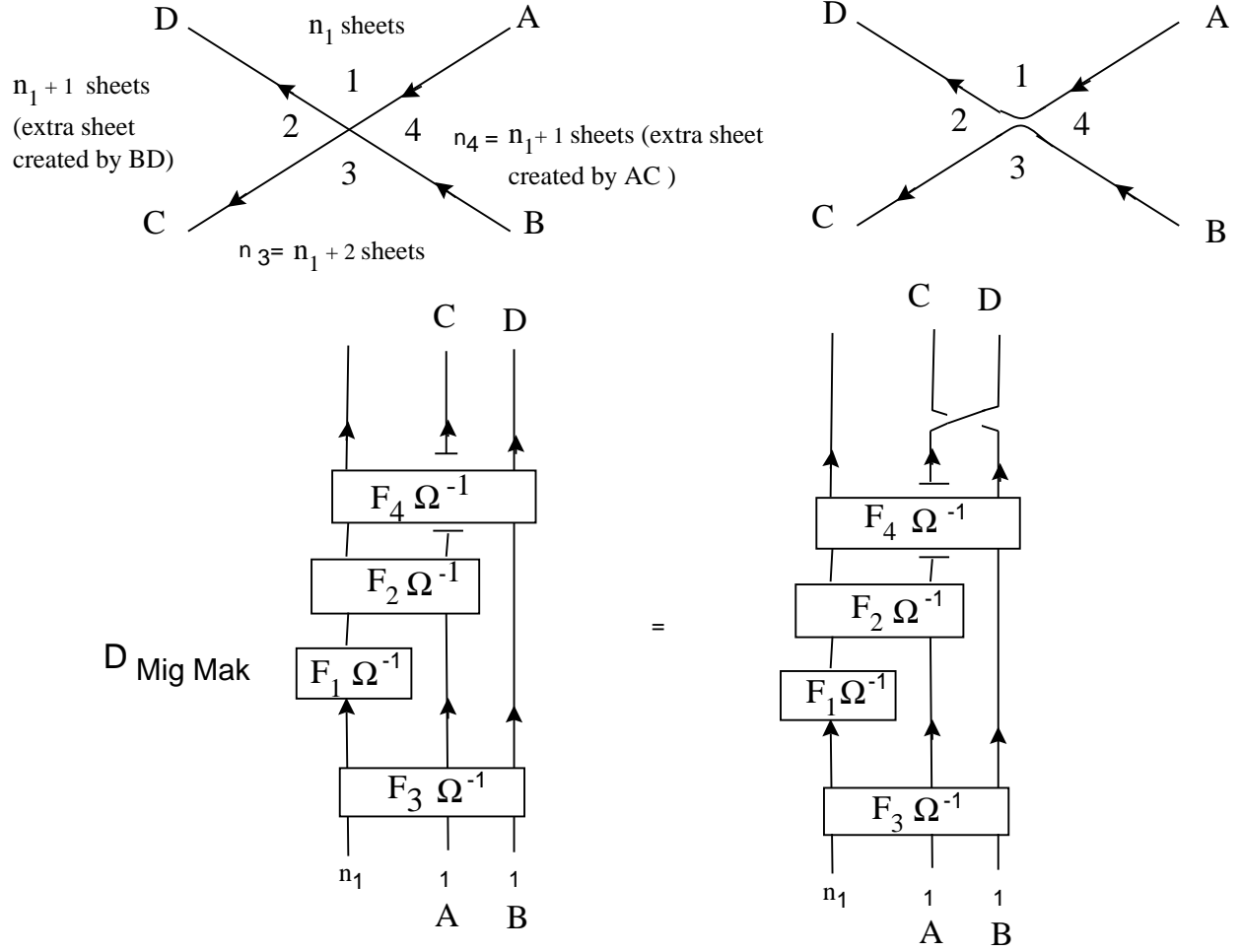


Fig. 27: Proof of Loop Equations.

the delta function for the Wilson average, to the pattern of embeddings shown. The sheet bounded by the side BD covers regions 2 and 3 and the corresponding strand is acted on by the F factors for these regions. The sheet bounded by the side AC covers regions 3 and 4 and so the corresponding sheet is acted on by F_3 and F_4 . Now if we act by the differential operator

$$D_{MigMak} = \frac{N\partial}{\partial A_2} + \frac{N\partial}{\partial A_4} - \frac{N\partial}{\partial A_1} - \frac{N\partial}{\partial A_3} + \frac{1}{N}. \quad (11.1)$$

(If we are doing the chiral zero charge sector of the $U(N)$ theory, we can drop the $1/N$ to give a simpler differential equation). It is an easy check, using the form of the F factors in (3.6), that the only contribution comes from $T_2^{(n_3)} + T_2^{(n_1)} - T_2^{(n_2)} - T_2^{(n_4)}$, where the T_2' s are sums of permutations in S_{n_1} to S_{n_4} , all embedded in S_{n_1+2} as shown in the figure, e.g

S_{n_4} acts on the first n_1 and the last strand. This difference of operators is just equal to the transposition which switches the last two sheets:

$$\begin{aligned}
& T_2^{(n_3)} + T_2^{(n_1)} - T_2^{(n_2)} - T_2^{(n_4)} \\
&= \sum_{i < j=1}^{n_1+2} (ij) + \sum_{i < j=1}^{n_1} (ij) - \sum_{i < j=1}^{n_1+1} (ij) - \sum_{i < j \in \{1 \dots n_1\} \cup \{n_1+2\}} (ij) \\
&= (n_1 + 1 \ n_1 + 2).
\end{aligned} \tag{11.2}$$

Transpositions acting on the first n_1 sheets occur twice with a plus sign from $T_2^{(n_1)}$ and $T_2^{(n_3)}$, and twice with a minus sign from $T_2^{(n_2)}$ and $T_2^{(n_4)}$. Transpositions that mix the strand labelled A (the $(n_1 + 1)$ ' st strand) with the first n_1 cancel because of positive contribution from $T_2^{(n_3)}$ and negative contribution from $T_2^{(n_4)}$. Transpositions that mix the strand labelled B with the first n_1 cancel due to contributions from $T_2^{(n_3)}$ and $T_2^{(n_4)}$. So we are left just with the transposition mixing the last two strands from $T_2^{(n_3)}$. But the resulting braid diagram is exactly what one would construct for the Wilson average on the upper right of fig. 27.

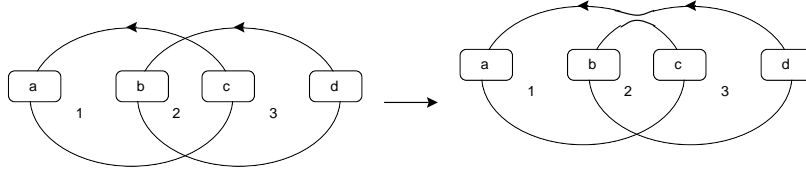


Fig. 28: First order differential operator acting on Wilson loop the left gives the Wilson loop on the right

In making an identification between certain points on the Wilson graph and certain strands of the braid diagram, we have used some physical intuition. We have seen from the construction of the braid diagram that it contains strands which start off being diagrammatic representations of the path traced by the Wilson line. Physically (as is obvious in a Hamiltonian quantization on a cylinder [20,21]) the Wilson observable creates a world-sheet boundary which propagates to form part of a covering of the manifold. To make the argument completely mathematical, we can analyze the structure of the braid diagram for some very general classes of Wilson loops. For example suppose we have two Wilson loops which intersect at the upper intersection of fig. 28. Since they are two distinct closed loops, they must intersect at least one more time. So quite generally we have the structure of fig. 28 where another intersection is shown as the lower one. The boxes indicate some

arbitrary windings. Note that in each region there may be some handles attached. For such a class of Wilson loops, one constructs the basic structure of the braid diagram, and shows that the above argument goes through : namely that the pattern of embeddings is the one shown in fig. 27, and that the remaining transposition obtained after acting with D_{MigMak} is exactly the one needed to give the braid diagram for the Wilson loop on the right of fig. 28.

Remarks :

1. There are also loop equations involving Wilson loops which have tangential intersections [22]. These can also be derived for the chiral theory using properties of the delta functions. The derivation for the case when the intersection is transversal involved the additive structure of classes of symmetric groups embedded in different ways in S_∞ (the group of permutations of all the natural numbers). The derivation in the case of tangential intersections involves the multiplicative structure in the algebra $\mathbb{Z}(S_\infty) \otimes \mathbb{R}(1/N)$. For example if Ω_{n_0} acts on integers 1 to n_0 , and Ω_{n_0+1} acts on integers 1 through $n_0 + 1$, then we have:

$$(1 + \sum_{i=1}^{n_0} \frac{(i n_0 + 1)}{N}) \Omega_{n_0} = \Omega_{n_0+1}. \quad (11.3)$$

2. The Loop equations are of course true for the correct large N expansion of 2d qcd (the coupled expansion). This does not contradict the fact that the Wilson average at large N is determined by the loop equations *given the correct boundary conditions*. The boundary conditions, i.e the Wilson averages for the non-intersecting non-overlapping Wilson loops, are in general different between chiral and non-chiral theory. Consider non-chiral Wilson Loops on the plane. In the non-chiral theory, for a collection of non-overlapping non-intersecting Wilson averages, the expectation value is just the product of $e^{-A_i/2}$ where the A_i are areas enclosed by the Wilson loops. In the chiral theory, there is also *a simple way to characterize the boundary conditions* : we have $e^{-A_i/2}$ for Wilson loops with orientation compatible with that induced by the region inside, which we call the plus orientation, and zero for Wilson Loops with the opposite orientation. If a Wilson loop can be reduced by the Loop equations to a collection of circles which all have the plus orientation, then chiral and non-chiral theory have the same boundary condition, and give the same answer. This can be understood from the string picture by using the rule [1] that, in the non-chiral theory, each Wilson loop can bound an orientation preserving sheet on the left or an orientation reversing sheet on the right. We see that only orientation preserving sheets are allowed, since the right of a loop is always the outside which has infinite area and therefore cannot have any sheets. So it is not surprising that for this class of Wilson loops chiral and non-chiral theory give the same answer.

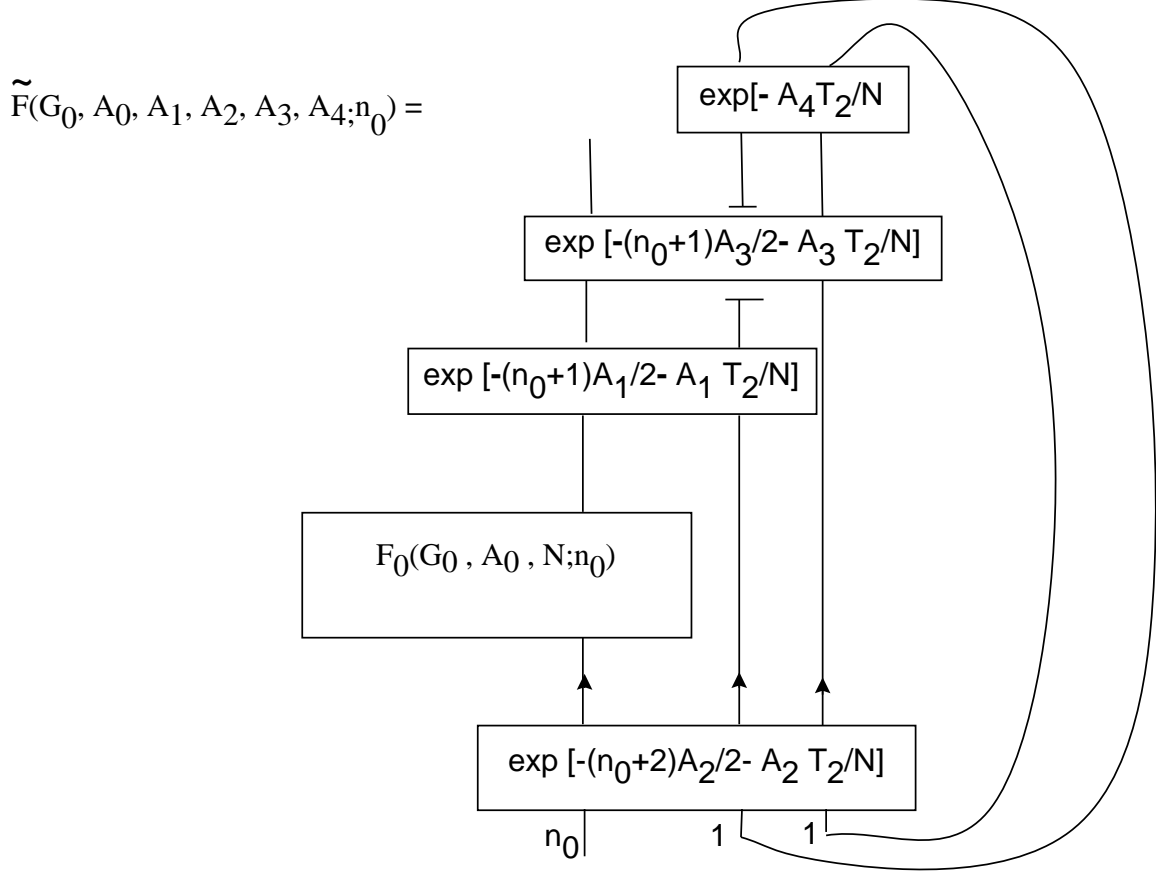


Fig. 29: Loop equations as constraints

12. Loop equations as linear constraints on the partition function

We have an expression for the loop equation as a relation between sets of operators acting on tensor spaces. We now show that the loop equations can be used to write first order differential equations for perturbations of the partition function.

Consider $\frac{1}{N^2} \tilde{F}(A_0, A_1, A_2, A_3, A_4; n_0)$ of fig. 29 as an operator on $V^{\otimes n_0}$. For any A_i it can be proved that this operator commutes with $U(N)$ acting on $V^{\otimes n_0}$ and also with S_{n_0} , so it must be possible to expand it in terms of casimirs acting on $V^{\otimes n_0}$, which would be the more usual way of describing deformations of the partition function [10,23].

Consider

$$Z(G_0, A_0, A_1, A_2, A_3, A_4) = \sum_{n_0} Z(G_0, A_0, A_1, A_2, A_3, A_4; n_0), \quad (12.1)$$

where

$$Z(G_0, A_0, A_1, A_2, A_3, A_4; n_0) = \text{tr}_{n_0} \left(\frac{\tilde{F}(G_0, A_0, A_1, A_2, A_3, A_4; n_0)}{N^2} \right). \quad (12.2)$$

If $A_i = 0$ for $(i = 1, \dots, 4)$, Z is equal to the term in the partition function for a target of area A_0 , with G_0 handles. For $A_4 = 0$ (other $A_i \neq 0$) the trace of the operator is the expectation value of the Wilson average for a pair of rings intersecting in two points as in fig. 24 and carrying the fundamental representation ($m_1 = m_2 = 1$). The derivative $\frac{-\partial Z(G_0, A_0, A_1, A_2, A_3, A_4)}{\partial A_4}|_{A_4=0}$ gives the Wilson loop resulting from applying the Migdal-Makeenko equation at the upper intersection of fig. 24. The derivative brings down the transposition shown alongside F_0 in fig. 20. The key cancellation of transpositions responsible for the Migdal-Makeenko equation can be expressed as a differential equation for $Z(G_0, A_i; n_0)$

$$\left[-\frac{\partial}{\partial A_0} - \frac{\partial}{\partial A_2} + \frac{\partial}{\partial A_1} + \frac{\partial}{\partial A_3} + \frac{\partial}{\partial A_4}\right] Z(G_0, A_i; n_0) = 0, \quad (12.3)$$

which results in the same equation for $Z(G_0, A_i)$. By introducing one extra area, like A_4 here, we can always write the Migdal-Makeenko equation as a differential operator annihilating a braid diagram. In general the braid diagram will not reduce to the partition function when the areas go to zero, but rather to the partition function with insertions of some local operators.

So we find a close analogy to 2D gravity : loop equations are equivalent to differential operator constraints on perturbations of the partition function. This was conjectured in section 9 of [2]. The surprise is that this is true for the **chiral** theory where the partition function has a geometrical interpretation as the generating function of orbifold Euler characters of classical Hurwitz spaces. It was further conjectured that the algebra satisfied by the constraints is W_∞ . The only algebra we have used is $\mathbb{Z}(S_\infty) \otimes \mathbb{R}(1/N)$. It would be interesting if this algebra could be related to W_∞ in a meaningful way.

While one side of the Migdal-Makeenko equations is of course linear, the other side contains a product of Wilson loops. So, expressed in the space of Wilson loops, the Migdal-Makeenko equations are non-linear. But we find that replacing “the space of Wilson loops” by “the space of delta functions over S_∞ , parametrised by area perturbations”, linearises the loop equations completely. It is an interesting question whether this can be done in higher dimensions.

13. General remarks

13.1. Finite N

We have focused on the chiral large N expansions for $U(N)$ and $SU(N)$. For finite N one can still use the same diagrammatic form to express the exact answer : only the exact formulae for converting the integrals into symmetric group data are different and haven't been fully worked out. In addition, there are some extra projection operators introduced in [24].

If n_0 is kept small and fixed, (e.g by having outside area equal to infinity which sets $n_0 = 0$ or by choosing to work with a manifold where one region has an extra boundary where the boundary condition is chosen to ensure fixed n_0 with $N \gg n_0$), and if the windings and $n(\vec{k}_\Gamma)$ of the Wilson loops are less than N , then the formulae we have already derived can be directly applied.

$$\int \text{U}^N = \sum_{\sigma} \frac{(-1)^{p(\sigma)}}{N!} \text{σ}^N$$

Fig. 30: an example $su(N)$ integral at finite N .

For $SU(N)$ at finite N , there is another subtlety in addition to projection operators. For n_1 and n_2 not necessarily small compared to N , the integral is no longer proportional to δ_{n_1, n_2} but rather to $\delta_{n_1, n_2 \bmod N}$ (see [25]). For example if $n_1 = N, n_2 = 0$ we can compute the integral by using the fact that the integral is the projector onto the identity representation. But the Young diagram with 1 column of length N is isomorphic to the identity representation, so we can use the formula for a projector onto a Young diagram Y

$$P_Y = d_{r(Y)} \sum_{\sigma \in S_n} \frac{1}{n!} \chi_{r(Y)}(\sigma^{-1}) \sigma. \quad (13.1)$$

For the relevant Y we have $d_{r(Y)} = 1$, $\chi_{r(Y)}(\sigma^{-1}) = (-1)^{p(\sigma)}$ where $p(\sigma)$ is the parity of the permutation σ . This leads to the formula in fig. 30 where the permutations summed are in S_N , in agreement with eq. 21 of [26]. It should be possible to write a general formula for this integral in the case of $SU(N)$, in terms of a sum over permutations, for arbitrary n_1 and n_2 . This might be useful in the calculation of correlation functions in interacting fermion systems [27] .

Since the basic structure of the braid diagram is unchanged, similar proofs to the one we described for the loop equations should be applicable at finite N .

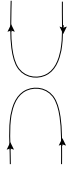


Fig. 31: Contraction operators

13.2. Non-chiral Theory

The method for writing and interpreting Wilson averages developed in this paper should generalise to the non-chiral theory. So far the main ingredient in the diagram has been a sequence of upward directed strands, which are acted on by permutations. The reason why we have only permutations is that the commutant of $SU(N)$ in $V^{\otimes n}$ is S_n . In the non-chiral theory we have to deal with $V^{\otimes n} \otimes \bar{V}^{\otimes m}$. Now the commutant is not just $S_n \times S_m$. Rather it includes the dual pairing of a vector and its dual in the complex conjugate representation. A generalisation of our construction would contain upward and downward strands, acted on by permutations and with operators like those in fig. 31. It is clear that these contraction operators will be needed: for example they allow us to write the coupled Loop functions of [1] as a trace of U acting in $V^{\otimes n} \otimes \bar{V}^{\otimes m}$. However the combinatorics of these contraction operators needs to be related to that of tubes in the coupled omega factor in order to solve the problem of describing the covering space geometry of Coupled intersecting Wilson loops. For arbitrary non-intersecting Wilson loops the details of the contraction operators can be bypassed, to write a general formula in terms of sums over symmetric groups. This formula is given and its relation to Euler characters of spaces of branched covers is discussed in [28] (see also [29]).

13.3. Higher dimensions

Reformulations of strong coupling expansions of higher dimensional lattice gauge theories in terms of surfaces have been made [30,31]. It was observed that the resulting statistical mechanics of surfaces is rather peculiar, not all surfaces are weighted by positive signs, and the weights are generally rather complicated. One source of minus signs is the Ω_n^{-1} factor which appears in fig. 18. In the context of the chiral expansion this leads to the Ω_n^{2-2G} for the genus G partition function (the chiral Gross Taylor expansion can be obtained rather directly from the heat kernel plaquette action for the standard cell decomposition of the Riemann surface into 1 two cell, one 0-cell and $2G$ 1-cells, and the integral of fig. 18) . But the story of YM_2 shows that all the weights and signs, at least in the chiral expansion, can be understood by thinking about the topology (Euler characters) of the space of branched covers. So we may naturally ask if the weights for surfaces in higher dimensional lattice gauge theory can be understood in terms of Euler characters of a space of branched covers.

It is probably best to approach this question by using the heat kernel action [32,5] as the plaquette action, and try to imitate the kind of expansion that was done in 2D QCD. This will involve the coupled expansion which comes from putting together chiral and antichiral in the right way. Here we will discuss the chiral sector which gives part of the full large N expansion. A delta function over symmetric groups can be derived for any coupling, giving the chiral expansion in terms of symmetric group data, but the hope of relating to Euler characters exists when we can ignore everything but the Ω factors: whether there is a sensible physical regime (analogous to the zero coupling (area) limit of YM_2) where this is justified is an important question which we will not address here, rather we will proceed formally taking as our starting point the heat kernel action with the exponent set to zero. The techniques for integration which we used in section 7 can be used in higher dimensions. We make some comments on the properties of the delta functions over symmetric groups which can be derived from such an approach.

For concreteness we have in mind the D -dimensional Eguchi-Kawai model (in which spacetime has the topology of a D -torus). Our remarks also apply to an arbitrary cell complex, where the plaquette action is put on the two-cells and group variables are attached to the 1-cells (this rather general set-up for relating lattice gauge theory to topology has been discussed in a different context by Boulatov [33]). The analog of the Wilson graph of previous sections is now the 1-skeleton (set of 0 and 1-cells) of the EK complex, consisting

of one vertex and D edges. By expanding the plaquette actions we have sums over integers n_{ij} for the plaquettes ($i < j$ running from 1 to D). These sums can be converted to symmetric group data in the standard way, giving 1 Ω factor each. The actual integral is over D independent variables, each giving an Ω^{-1} factor according to fig. 18. After doing these integrals we are left with a trace in $V^{\otimes \sum_{i,j} 2n_{ij}}$ (the two comes from the operation of fig. 17) . It can be converted to a delta function by inserting an Ω factor using (2.6). So we have an Ω factor for each two-cell, an Ω^{-1} for each 1-cell, and an Ω factor which may be associated with the 0-cell. So the net number of Ω factors is equal to the Euler character of the 2-skeleton of the EK complex. As we saw for the partition function and Wilson loops the 2D analog of this fact was one of the important ingredients in showing that the zero coupling partition function in YM2 computes Euler characters of a space of branched covers. For more general complexes we have to contract the 1-skeleton, (as we did for Wilson graphs in previous sections) by using gauge invariance to one that has a single vertex (For EK we don't have to do this step since it is already a "reduced model"). We have seen that this contraction process does not change the Euler character of the 1-skeleton. It also does not change the number of 2-cells (closed loop variables bounding 2-cells cannot be gauged away). So it does not change the Euler character of the 2-skeleton. By the same argument as for the EK model then, the net number of Ω factors is equal to the Euler character of the two-skeleton of the cell complex. This motivates the following

Conjecture : The partition function for Lattice gauge theory with the zero area heat kernel action for a D -dimensional cell complex is the generating function for orbifold Euler characters of a space of branched covers of the 2 skeleton of the cell complex.

To account for the structure of the delta functions completely in terms of covering spaces, and to define precisely the relevant class of branched covers appears rather subtle: the mathematics of *branched* covers of arbitrary 2-complexes is not well-developed like that of ordinary surfaces. We may however expect many techniques to carry over : this is indicated for example by the fact that the chiral expansion for the EK complex (which is orientable) contains only even powers of N . Moreover one wants to explain from the geometrical point of view, not just the net number of Ω factors, but also their degrees. These issues are under investigation.

Acknowledgements

I thank G. Moore for many discussions and for collaboration on section 11. I thank S. Cordes, I. Frenkel, M. Henningson, R. Howe, R. Plesser, R. Puzio, S. Shatashvili, W.

Taylor for useful discussions. This work is supported by DOE grant DE-AC02-76ER03075, DOE grant DE-FG02-92ER25121.

Appendix A. Some properties of Braid Diagrams.

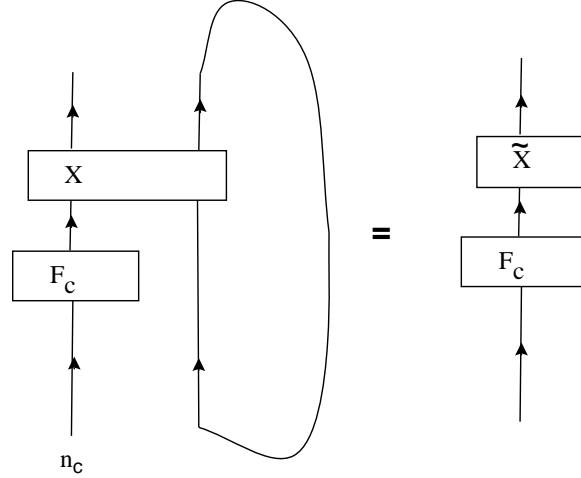


Fig. 32: generic operator

We discuss some properties of braid diagrams which are useful in manipulating them. Consider the n_c strands entering a given F_c . The remaining strands have been lumped, using the isomorphism shown in fig. 16, into the second strand of multiplicity l . The braid diagram appears as in fig. 32 where the X operator is the sequence of permutations, coming from other F factors, their conjugating factors, and from the windings of the Wilson loop. Having traced away the indices for the second strand, we are left with an operator on the first strand \tilde{X} . This operator commutes with the action of $SU(N)$ on $V^{\otimes n_c}$:

$$\begin{aligned}
 & (1 \otimes tr)(U \otimes 1)X \\
 &= (1 \otimes tr)(1 \otimes U^{-1})(U \otimes U)X \\
 &= (1 \otimes tr)(1 \otimes U^{-1})X(U \otimes U) \\
 &= (1 \otimes tr)X(U \otimes 1).
 \end{aligned} \tag{A.1}$$

Here we have used the fact that on $V^{\otimes(n_c+l)}$ the standard action of $SU(N)$ commutes with permutations. In the last line we used cyclicity of the trace. So \tilde{X} commutes with $SU(N)$. By Schur-Weyl duality it must be a permutation. More intuitively the strands from the first n_c wander through the second set of strands and come back with a permutation. It is often useful in proving properties of braid diagrams to use these commutativity properties, and to simplify the braid diagram to make manifest certain properties which do not use the full bulk of the braid diagram e.g for loop equations or for giving evidence, from this point of view, for the Gross-Taylor rule on the placing of Omega points.

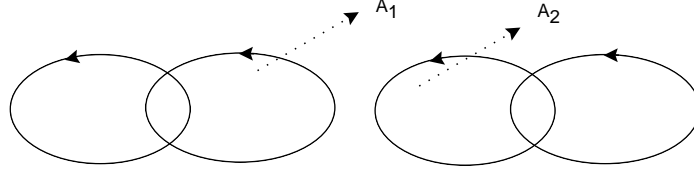


Fig. 33:

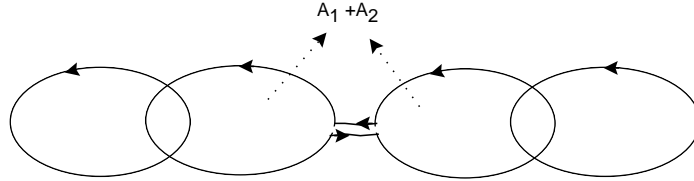


Fig. 34: connected sum of plane curves

Simple operations on braid diagrams are both natural and useful in expressing properties of Wilson loops. We can always combine delta functions for a Wilson average into 1 delta function even if the Wilson graph is disconnected. Suppose it has 2 components, as in the example in fig. 33 . Using the group integrals and the techniques we have described, one derives sums with 3 delta functions.

The form of the answer is shown in fig. 35. There are sums over n_0 and permutations u_1 and u_2 in S_{n_0} . Solving the delta functions gives a single delta function, which is a *connected sum* of the braid diagrams we would have for the two Wilson loops separately. In case n_0 is zero we have a trivial concatenation into a single delta function on of permutations of $m_1 + m_2$ integers, where the permutations have the property of lying in the subgroup $S_{m_1} \times S_{m_2}$. It is clear from the covering space geometry that we should always be able to write a single delta function, with different permutations associated with different paths on the same manifold. This point is important in expressing both left and right hand side of Migdal-Makeenko equations as linear operators on a single delta function, as we did in section 12.

Connected sums of braid diagrams (these are studied in knot theory e.g [34]) are also useful in proving relations between different Wilson loops. For example consider the set of Wilson loops in fig. 34, which is a connected sum of those in fig. 33 (here we are using connected sums of curves in the sense used for example in [35]). Suppose we are working in the representation basis and that the outside area is infinite. Then this Wilson average of fig. 34 equal to the Wilson average for fig. 33 divided by dimension of

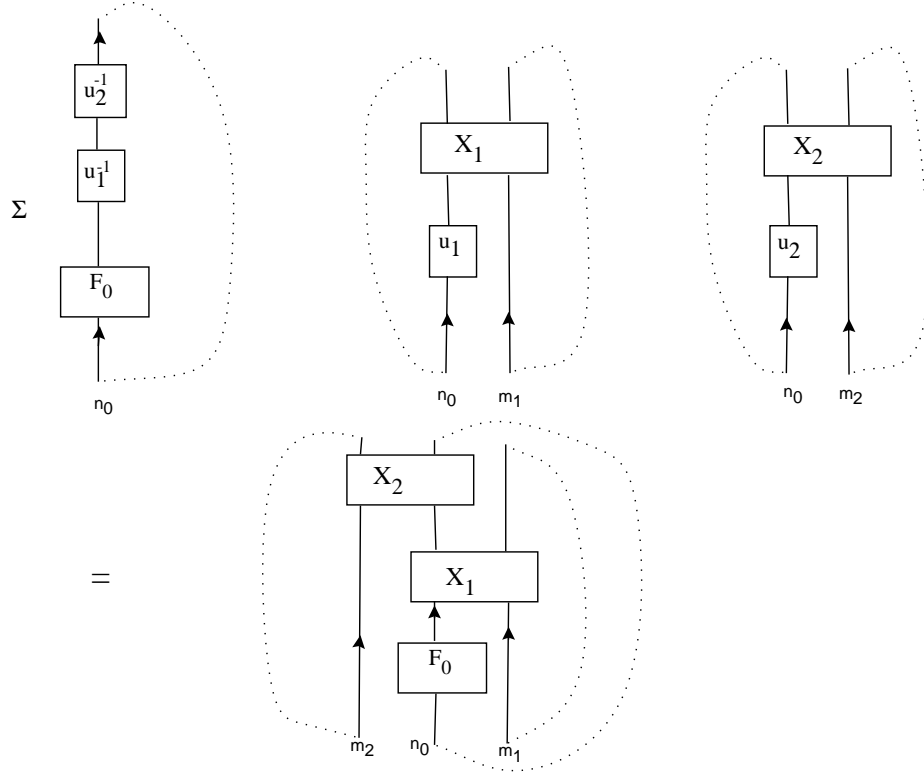


Fig. 35: Lower braid diagram has structure of connected sum of the two on upper right

the representation R carried by the middle circle of fig. 34. The $\dim R$ factor is simply understood from the Euler character point of view by counting the Euler character of the space over which the branch points are allowed to move. This relation between the expectation value of connected sums of Wilson loops and the original Wilson loops (when outside area is infinite) is very general and the proof based on forming connected sums of braid diagrams can also be applied at finite N .

References

- [1] D. Gross, “Two Dimensional QCD as a String Theory”, Nucl. Phys. **B400** (1993) 161, hep-th/9212149.; D. Gross and W. Taylor, “Two-dimensional QCD is a String Theory”, Nucl. Phys. **B400** (1993) 181, hep-th/93011068; D. Gross and W. Taylor, “Twists and Loops in the String Theory of Two Dimensional QCD”, Nucl. Phys. **403** (1993) 395, hep-th/9303046.
- [2] S. Cordes, G. Moore, and S. Ramgoolam, “Large N 2D Yang-Mills Theory and Topological String Theory”, hep-th/9402107.
- [3] E. Witten, “On Quantum gauge theories in two dimensions,” Commun. Math. Phys. **141** (1991) 153.
- [4] B. Rusakov, “Loop Averages And Partition Functions in $U(N)$ Gauge Theory On Two-Dimensional Manifolds”, Mod. Phys. Lett. **A5** (1990) 693.
- [5] A. Migdal, “Recursion Relations in Gauge Theories”, Zh. Eksp. Teor. Fiz. **69** (1975) 810 (Sov. Phys. JETP. **42** 413).
- [6] E. Verlinde and H. Verlinde, “A Solution of Two-Dimensional Topological Quantum Gravity”, Nucl. Phys. **B348** (1991) 457, R. Dijkgraaf, E. Verlinde and H. Verlinde, “Loop Equations and Virasoro Constraints in Nonperturbative 2d Quantum Gravity”, Nucl. Phys. **B348** (1991) 435; “Topological Strings in $d < 1$ ”, Nucl. Phys. **B352** (1991) 59; “Notes on Topological String Theory and 2-d Quantum Gravity”, in *String Theory and Quantum Gravity*, Proc. Trieste Spring School, April 24 - May 2, 1990 (World Scientific, Singapore, 1991).
- [7] M. Douglas and V.A. Kazakov, “Large N Phase Transition in Continuum QCD₂”, Phys. Lett. **B319** (1993) 219, hep-th/9305047
- [8] R. Rudd, “The String Partition Function for QCD on the Torus”, hep-th/9407176.
- [9] M. Crescimanno and W. Taylor, “Large N phases of Chiral QCD₂,” hep-th 9408115.
- [10] S. Cordes, G. Moore, and S. Ramgoolam, in Les Houches Session LXII on <http://xxx.lanl.gov/lh94>.
- [11] D. P. Zhelobenko, Translations of American Math. Monographs, **40**.
- [12] J. Minahan, “Summing over Inequivalent Maps in the String Theory of QCD”, Phys. Rev. **D47** (1993) 3430.
- [13] C. L. Ezell, “Branch Point Structure of Covering Maps onto Nonorientable Surfaces”, Transactions of the American Mathematical society, vol **243**, 1978.
- [14] I.K. Kostov, “Continuum QCD₂ in Terms of Discretized Random Surfaces with Local Weights”, Saclay-SPht-93-050; hep-th/9306110.
- [15] H. Seifert and W. Threlfall, “A textbook of Topology,” translated by M.A. Goldman, Academic press 1980.
- [16] G. Moore and N. Seiberg, “Polynomial Equations for Rational Conformal Field Theories,” Phys. Lett. **212B**(1988)451; “Classical and Quantum Conformal Field Theory”,

- Commun. Math. Phys. **123**(1989)177; “Lectures on Rational Conformal Field Theory”, in *Strings 90*, the proceedings of the 1990 Trieste Spring School on Superstrings.
- [17] N. Reshetikhin and V.G. Turaev, “Invariants of three-manifolds via link polynomials and quantum groups,” Invent. math. 103 (1991).
 - [18] N. Reshetikhin, “Quasitriangular Hopf algebras and invariants of links,” Algebra and Analysis, v.1, N2, (1990).
 - [19] W.S. Massey, *A Basic Course in Algebraic Topology*, Springer-Verlag, 1991.
 - [20] J. Minahan and A. Polychronakos, “Equivalence of Two Dimensional QCD and the $c = 1$ Matrix Model”, Phys. Lett. **B312** (1993) 155; hep-th/9303153.
 - [21] M.R. Douglas, “Conformal Field Theory Techniques for Large N Group Theory,” hep-th/9303159; M.R. Douglas, “Conformal Field Theory Techniques in Large N Yang-Mills Theory”, hep-th/9311130, to be published in the proceedings of the May 1993 Cargèse workshop on Strings, Conformal Models and Topological Field Theories.
 - [22] V.A. Kazakov and I. Kostov, “Non-linear Strings in Two-Dimensional $U(\infty)$ Gauge Theory,” Nucl. Phys. **B176** (1980) 199-215; “Computation of the Wilson Loop Functional in Two-Dimensional $U(\infty)$ Lattice Gauge Theory”, Phys. Lett. **B105** (1981) 453; V.A. Kazakov, “Wilson Loop Average for an Arbitrary Contour in Two-Dimensional $U(N)$ Gauge Theory”, Nuc. Phys. **B179** (1981) 283-292.
 - [23] O. Ganor, J. Sonnenschein, S. Yankielowicz, ” The string theory approach to 2D Yang Mills Theory, ” Jul 1994, hep-th 9407114
 - [24] J. Baez and W. Taylor, ”Strings and Two-dimensional QCD for Finite N ”, MIT-CTP-2266, hep-th/9401041.
 - [25] J.M. Drouffe and J. B. Zuber, “Strong Coupling and Mean Field Methods in Lattice Gauge theories”, Phys. Rept **102** (1983) 1.
 - [26] M. Creutz, “ On invariant integration over $SU(N)$, ” J. Math. Phys. **19** (10), October 1978.
 - [27] J. Minahan and A. Polychronakos, ”Interacting Fermion Systems from Two Dimensional QCD”, Phys. Lett. **326** (1994) 288; hep-th/9309044.
 - [28] S. Ramgoolam, “Coupled non-intersecting Loops in 2D Yang Mills and free fields, ” YCTP-P18-94.
 - [29] S.G.Naculich, H.A.Riggs, “The String Calculation of QCD Wilson loops on arbitrary surfaces,” hep-th 9411143.
 - [30] K.H. O’Brien and J.-B. Zuber, “Strong Coupling Expansion of Large N QCD and Surfaces”, Nucl. Phys. **B253** (1985) 621.
 - [31] V.A. Kazakov, “ $U(\infty)$ Lattice Gauge Theory as a Free Lattice String Theory”, Phys. Lett. **B128** (1983) 316; V.I. Kostov, “Multicolour QCD in Terms of Random Surfaces”, Phys. Lett. **B138** (1984) 191.
 - [32] P. Menotti and E. Onofri, “The action of $SU(N)$ lattice gauge theory in terms of the eat kernal on the group manifold, ” NPB190: 288. 1981.

- [33] D.V. Boulatov : “ q-deformed lattice gauge theory and 3 manifold invariants, ” Hephth 9210032, Int. J. Mod.Phys. A8: 3139-3162, 1993.
- [34] L.H. Kauffmann, “Knots and Physics, ” World Scientific 1991.
- [35] See V. Arnold, “Remarks on Enumeration of Plane Purves”; “Plane Curves, their Invariants, Perestroikas and Classifications”.